ΠΑΝΕΠΙΣΤΗΜΙΟ ΚΡΗΤΗΣ
ΔΙΑΤΜΗΜΑΤΙΚΟ ΜΕΤΑΠΤΥΧΙΑΚΟ
ΠΡΟΓΡΑΜΜΑ ΣΠΟΥΔΩΝ
ΟΠΤΙΚΗ ΚΑΙ ΟΡΑΣΗ

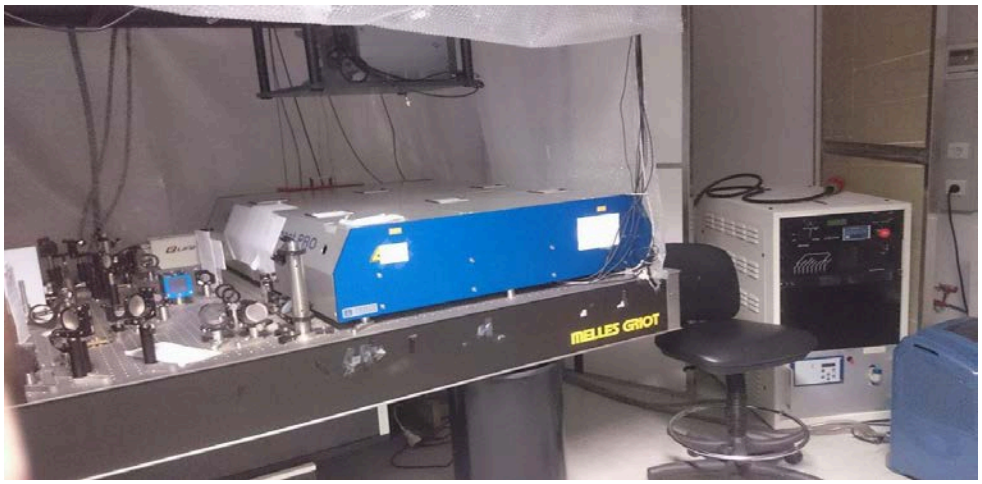

Absorption and fluorescence spectroscopy of biological tissues, by using intense pulsed laser, in order to detect differences between pathological and healthy tissues

Student: ***Psycharakis Panagiotis-Christos***

Supervisors: **Loukakos Panagiotis**, Principal Researcher, Foundation for Research and Technology – Hellas, Institute of Electronic Structure and Laser.

Tsilibaris Miltiadis, Professor, University of Crete, School of Medicine

Kymionis Georgios, Associate Professor, National and Kapodistrian University of Athens, Health Sciences, Faculty of Medicine

Pallikaris Aristofanis, BioMedical Engineer, Research assistant, Institute of Vision and Optics

Acknowledgments

I would like to thank all the people from Foundation for Research and Technology – Hellas, from the university of Crete and from General Hospital of Heraklion (ΠΑΓΝΗ) who have supported me during the last months and whose contributions and suggestions enabled me to enhance my work at every stage. My gratitude is also directed towards my supervisors Dr. Loukakos Panagiotis (researcher at FORTH) who gave me the permission to use the equipment of his laboratory and especially the spectrometer and laser in order to to do my experiments and advised me in every step of my research, Prof. Kymionis Georgios (Professor at National and Kapodistrian University of Athens, Faculty of Medicine) who provided me with eye tissues and useful information, Mr. Pallikaris Aristofanis (BioMedical Engineer, Research Assistant at IVO) who gave me very important advices, Prof. Tsilimparis Miltiadis (Professor at University of Crete, School of Medicine) and Mr. Konstantinos Droutsas who provided me with eye tissues.

Finally, special thanks go to my parents and brother for supporting and motivating me in every single situation.

Contents

1. Introduction

The aim of this project is to measure the absorption and fluorescence spectroscopy of biological tissues in order to detect differences between pathological and healthy tissues. In order to achieve our goal we used special high technological machines which were provided to us by ITE. As far as the absorption spectroscopy is concerned we used perkin elmer lambda 950 spectrometer which is able to measure a wide range of spectre from 2500 nm to 25nm. As far as the fluorescence spectroscopy is concerned we carried out our measurements thanks to a powerful Laser that ITE posseses, the femtopower compact pro Laser.

Diagnostic techniques based on absorption and fluorescence spectroscopy have the potential to link the biochemical and morphologic properties of tissues to individual patient care. In particular, these techniques are fast, non-invasive and quantitative. Furthermore, they can be used to elucidate key tissue features, such as the cellular metabolic rate, vascularity, intra-vascular oxygenation and alterations in tissue morphology. These tissue features can be interpreted to shed light on a variety of clinical problems, such as neoplasia and atherosclerosis. If applied successfully, absorption and fluorescence spectroscopy has the potential to represent an important step forward toward advances in diagnostic and therapeutic medical applications

2. Theoretical Background

2.1. Basic Principles of Spectroscopy

History

The history of spectroscopy began with Isaac Newton's optics experiments (1666–1672). Newton applied the word "spectrum" to describe the rainbow of colors that combine to form white light and that are revealed when the white light is passed through a prism. During the early 1800s, Joseph von Fraunhofer made experimental advances with dispersive spectrometers that enabled spectroscopy to become a more precise and quantitative scientific technique. Since then, spectroscopy has played and continues to play a significant role in chemistry, physics and astronomy.

Spectroscopy

Spectroscopy is the study of the interaction between matter and electromagnetic radiation. Historically, spectroscopy originated through the study of

visible light dispersed according to its wavelength, by a prism. Later the concept was expanded greatly to include any interaction with radiative energy as a function of its wavelength or frequency. Spectroscopic data is often represented by an emission spectrum, a plot of the response of interest as a function of wavelength or frequency.

Introduction

Spectroscopy and spectrography are terms used to refer to the measurement of radiation intensity as a function of wavelength and are often used to describe experimental spectroscopic methods. Spectral measurement devices are referred to as spectrometers, spectrophotometers, spectrographs or spectral analyzers.

Daily observations of color can be related to spectroscopy. Neon lighting is a direct application of atomic spectroscopy. Neon and other noble gases have characteristic emission frequencies (colors). Neon lamps use collision of electrons with the gas to excite these emissions. Inks, dyes and paints include chemical compounds selected for their spectral characteristics in order to generate specific colors and hues. A commonly encountered molecular spectrum is that of nitrogen dioxide. Gaseous nitrogen dioxide has a characteristic red absorption feature, and this gives air polluted with nitrogen dioxide a reddish brown color. Rayleigh scattering is a spectroscopic scattering phenomenon that accounts for the color of the sky.

Spectroscopic studies were central to the development of quantum mechanics and included Max Planck's explanation of blackbody radiation, Albert Einstein's explanation of the photoelectric effect and Niels Bohr's explanation of atomic structure and spectra. Spectroscopy is used in physical and analytical chemistry because atoms and molecules have unique spectra. As a result, these spectra can be used to detect, identify and quantify information about the atoms and molecules. Spectroscopy is also used in astronomy and remote sensing on earth. Most research telescopes have spectrographs. The measured spectra are used to determine the chemical composition and physical properties of astronomical objects (such as their temperature and velocity).

Theory

One of the central concepts in spectroscopy is a resonance and its corresponding resonant frequency. Resonances were first characterized in mechanical systems such as pendulums. Mechanical systems that vibrate or oscillate will experience large amplitude oscillations when they are driven at their resonant frequency. A plot of amplitude vs. excitation frequency will have a peak centered at the resonance frequency. This plot is one type of spectrum, with the peak often referred to as a spectral line, and most spectral lines have a similar appearance.

In quantum mechanical systems, the analogous resonance is a coupling of two quantum mechanical stationary states of one system, such as an atom, via an oscillatory source of energy such as a photon. The coupling of the two states is strongest when the energy of the source matches the energy difference between the two states. The energy (E) of a photon is related to its frequency (ν) by:

$$E=h\nu$$

where (h) is Planck's constant, and so a spectrum of the system response vs. photon frequency will peak at the resonant frequency or energy. Particles such as electrons and neutrons have a comparable relationship, the de Broglie relations, between their kinetic energy and their wavelength and frequency and therefore can also excite resonant interactions.

Spectra of atoms and molecules often consist of a series of spectral lines, each one representing a resonance between two different quantum states. The explanation of these series, and the spectral patterns associated with them, were one of the experimental enigmas that drove the development and acceptance of quantum mechanics. The hydrogen spectral series in particular was first successfully explained by the Rutherford-Bohr quantum model of the hydrogen atom. In some cases spectral lines are well separated and distinguishable, but spectral lines can also overlap and appear to be a single transition if the density of energy states is high enough. Named series of lines include the principal, sharp, diffuse and fundamental series.

Classification of methods

Spectroscopy is a sufficiently broad field that many sub-disciplines exist, each with numerous implementations of specific spectroscopic techniques. The various implementations and techniques can be classified in several ways.

➢ Type of radiative energy

Types of spectroscopy are distinguished by the type of radiative energy involved in the interaction. In many applications, the spectrum is determined by measuring changes in the intensity or frequency of this energy. The types of radiative energy studied include:

- **Electromagnetic radiation** was the first source of energy used for spectroscopic studies. Techniques that employ electromagnetic radiation are typically classified by the wavelength region of the spectrum and include microwave, terahertz, infrared, near infrared, visible and ultraviolet, x-ray and gamma spectroscopy.
- Particles, due to their **de Broglie wavelength**, can also be a source of radiative energy and both electrons and neutrons are commonly used. For a particle, its kinetic energy determines its wavelength.
- **Acoustic spectroscopy** involves radiated pressure waves.
- **Mechanical** methods can be employed to impart radiating energy, similar to acoustic waves, to solid materials.

➢ Nature of the interaction

Types of spectroscopy can also be distinguished by the nature of the interaction between the energy and the material. These interactions include:

- **Absorption** occurs when energy from the radiative source is absorbed by the material. Absorption is often determined by measuring the fraction of energy transmitted through the material; absorption will decrease the transmitted portion.

- **Emission** indicates that radiative energy is released by the material. A material's blackbody spectrum is a spontaneous emission spectrum determined by its temperature; this feature can be measured in the infrared by instruments such as the Atmospheric Emitted Radiance Interferometer (AERI).[4] Emission can also be induced by other sources of energy such as flames or sparks or electromagnetic radiation in the case of fluorescence.
- **Elastic scattering** and reflection spectroscopy determine how incident radiation is reflected or scattered by a material. Crystallography employs the scattering of high energy radiation, such as x-rays and electrons, to examine the arrangement of atoms in proteins and solid crystals.
- **Impedance spectroscopy** studies the ability of a medium to impede or slow the transmittance of energy. For optical applications, this is characterized by the index of refraction.
- **Inelastic scattering** phenomena involve an exchange of energy between the radiation and the matter that shifts the wavelength of the scattered radiation. These include Raman and Compton scattering.
- **Coherent or resonance spectroscopy** are techniques where the radiative energy couples two quantum states of the material in a coherent interaction that is sustained by the radiating field. The coherence can be disrupted by other interactions, such as particle collisions and energy transfer, and so often require high intensity radiation to be sustained. Nuclear magnetic resonance (NMR) spectroscopy is a widely used resonance method and ultrafast laser methods are also now possible in the infrared and visible spectral regions.

➢ Type of material

Spectroscopic studies are designed so that the radiant energy interacts with specific types of matter.

Atoms

Atomic spectroscopy was the first application of spectroscopy developed. Atomic absorption spectroscopy (AAS) and atomic emission spectroscopy (AES) involve visible and ultraviolet light. These absorptions and emissions, often referred to as atomic spectral lines, are due to electronic transitions of outer shell electrons as they rise and fall from one electron orbit to another. Atoms also have distinct x-ray spectra that are attributable to the excitation of inner shell electrons to excited states.

Atoms of different elements have distinct spectra and therefore atomic spectroscopy allows for the identification and quantitation of a sample's elemental composition. Robert Bunsen and Gustav Kirchhoff discovered new elements by observing their emission spectra. Atomic absorption lines are observed in the solar spectrum and referred to as Fraunhofer lines after their discoverer. A comprehensive

explanation of the hydrogen spectrum was an early success of quantum mechanics and explained the Lamb shift observed in the hydrogen spectrum, which further led to the development of quantum electrodynamics.

Modern implementations of atomic spectroscopy for studying visible and ultraviolet transitions include flame emission spectroscopy, inductively coupled plasma atomic emission spectroscopy, glow discharge spectroscopy, microwave induced plasma spectroscopy, and spark or arc emission spectroscopy. Techniques for studying x-ray spectra include X-ray spectroscopy and X-ray fluorescence (XRF).

Molecules

The combination of atoms into molecules leads to the creation of unique types of energetic states and therefore unique spectra of the transitions between these states. Molecular spectra can be obtained due to electron spin states (electron paramagnetic resonance), molecular rotations, molecular vibration and electronic states. Rotations are collective motions of the atomic nuclei and typically lead to spectra in the microwave and millimeter-wave spectral regions; rotational spectroscopy and microwave spectroscopy are synonymous. Vibrations are relative motions of the atomic nuclei and are studied by both infrared and Raman spectroscopy. Electronic excitations are studied using visible and ultraviolet spectroscopy as well as fluorescence spectroscopy.

Studies in molecular spectroscopy led to the development of the first maser and contributed to the subsequent development of the laser.

Crystals and extended materials

The combination of atoms or molecules into crystals or other extended forms leads to the creation of additional energetic states. These states are numerous and therefore have a high density of states. This high density often makes the spectra weaker and less distinct, i.e., broader. For instance, blackbody radiation is due to the thermal motions of atoms and molecules within a material. Acoustic and mechanical responses are due to collective motions as well. Pure crystals, though, can have distinct spectral transitions, and the crystal arrangement also has an effect on the observed molecular spectra. The regular lattice structure of crystals also scatters x-rays, electrons or neutrons allowing for crystallographic studies.

Nuclei

Nuclei also have distinct energy states that are widely separated and lead to gamma ray spectra. Distinct nuclear spin states can have their energy separated by a magnetic field, and this allows for NMR spectroscopy.

Other types

Other types of spectroscopy are distinguished by specific applications or implementations:

- **Acoustic resonance spectroscopy** is based on sound waves primarily in the audible and ultrasonic regions
- **Auger spectroscopy** is a method used to study surfaces of materials on a micro-scale. It is often used in connection with electron microscopy.
- **Cavity ring down spectroscopy**
- **Circular Dichroism spectroscopy**
- **Coherent anti-Stokes Raman spectroscopy (CARS)** is a recent technique that has high sensitivity and powerful applications for *in vivo* spectroscopy and imaging.
- **Cold vapour atomic fluorescence spectroscopy**
- **Correlation spectroscopy** encompasses several types of two-dimensional NMR spectroscopy.
- **Deep-level transient spectroscopy** measures concentration and analyzes parameters of electrically active defects in semiconducting materials
- **Dual polarisation interferometry** measures the real and imaginary components of the complex refractive index
- **Electron phenomenological spectroscopy** measures physicochemical properties and characteristics of electronic structure of multicomponent and complex molecular systems.
- **EPR spectroscopy**
- **Force spectroscopy**
- **Fourier transform spectroscopy** is an efficient method for processing spectra data obtained using interferometers. Fourier transform infrared spectroscopy (FTIR) is a common implementation of infrared spectroscopy. NMR also employs Fourier transforms.
- **Hadron spectroscopy** studies the energy/mass spectrum of hadrons according to spin, parity, and other particle properties. Baryon spectroscopy and meson spectroscopy are both types of hadron spectroscopy.
- **Hyperspectral imaging** is a method to create a complete picture of the environment or various objects, each pixel containing a full visible, VNIR, NIR, or infrared spectrum.
- **Inelastic electron tunneling spectroscopy (IETS)** uses the changes in current due to inelastic electron-vibration interaction at specific energies that can also measure optically forbidden transitions.
- **Inelastic neutron scattering** is similar to Raman spectroscopy, but uses neutrons instead of photons.
- **Laser-Induced Breakdown Spectroscopy (LIBS),** also called Laser-induced plasma spectrometry (LIPS)
- **Laser spectroscopy** uses tunable lasers and other types of coherent emission sources, such as optical parametric oscillators, for selective excitation of atomic or molecular species.
- **Mass spectroscopy** is an historical term used to refer to mass spectrometry. Current recommendations are to use the latter term. Use of the term mass spectroscopy originated in the use of phosphor screens to detect ions.

- **Mössbauer spectroscopy** probes the properties of specific isotopic nuclei in different atomic environments by analyzing the resonant absorption of gamma-rays. See also Mössbauer effect.
- **Neutron spin echo spectroscopy** measures internal dynamics in proteins and other soft matter systems
- **Photoacoustic spectroscopy** measures the sound waves produced upon the absorption of radiation.
- **Photoemission spectroscopy**
- **Photothermal spectroscopy** measures heat evolved upon absorption of radiation.
- **Pump-probe spectroscopy** can use ultrafast laser pulses to measure reaction intermediates in the femtosecond timescale.
- **Raman optical activity spectroscopy** exploits Raman scattering and optical activity effects to reveal detailed information on chiral centers in molecules.
- **Raman spectroscopy**
- **Saturated spectroscopy**
- **Scanning tunneling spectroscopy**
- **Spectrophotometry**
- **Time-resolved spectroscopy** measures the decay rate(s) of excited states using various spectroscopic methods.
- **Time-Stretch Spectroscopy**
- **Thermal infrared spectroscopy** measures thermal radiation emitted from materials and surfaces and is used to determine the type of bonds present in a sample as well as their lattice environment. The techniques are widely used by organic chemists, mineralogists, and planetary scientists.
- **Ultraviolet photoelectron spectroscopy (UPS)**
- **Ultraviolet–visible spectroscopy**
- **Vibrational circular dichroism spectroscopy**
- **Video spectroscopy**
- **X-ray photoelectron spectroscopy (XPS)**

2.2. Basic Principles of Anatomy and Physiology

Skin

With an approximate area of 2 m^2 and a weight of 10 kg, the skin is the biggest organ in the human body. Some of its functions are protection, sensation, temperature regulation, the production of vitamin D and excretion. The skin is

roughly divided in epidermis, dermis and hypodermis (Figure 2.1). The epidermis is the superficial part of the skin and acts as a barrier against microorganisms, chemicals, abrasion, UV-light and to prevent water loss. It also produces vitamin D, contains melanin and gives rise to hair, nails and glands. The dermisis below the epidermis and is responsible for the flexibility and structural strength of the skin. It also contains many lymph vessels and blood vessels because this is where a great part of the exchange with nutrients, gases and waste products takes place. Beside collagen, elastic fibers, nerve fibers, oil and sweat glands and hair follicles, the dermis also has melanin. The lowermost skin layer, the hypodermis, is mainly used for fat storage (adipose tissue) and has loosely dispersed elastic fibers. It also contains blood vessels, nerve fibers, and small amounts of melanin. Its main function is to avoid or slow heat loss. The structure of the skin varies along the body; for example the sole of the foot has an up to 2 mm thick layer, while some other parts are hairy and some others thin and hairless. Between the dermis and the epidermis there is a layer called papillary region, which is composed of elastic fibers, connective tissue, collagen and adipose tissue.

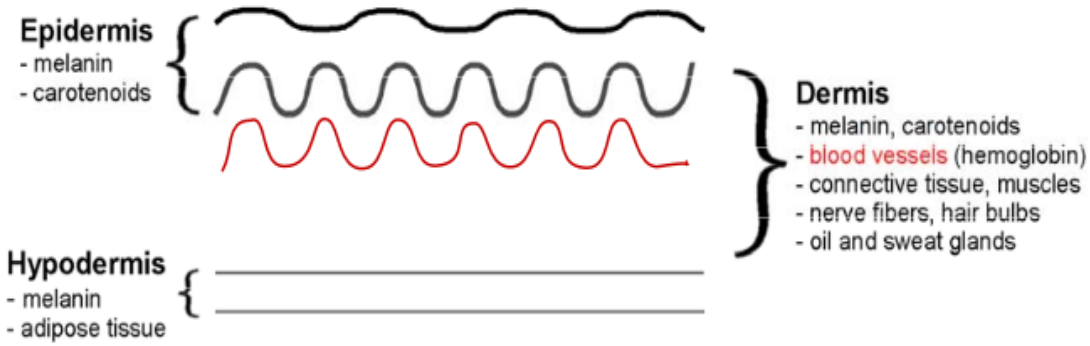

Figure 2.1 Structure and layers of the skin

Melanin, hemoglobin and carotene are the three pigments which contribute to skin color. All of them have a strong light absorption in the UV and blue wavelength. Only melaninis produced in the skin by melanocytes, and its color ranges from yellow to red-dish-brown to black. The largest amounts of melanin are located in the epidermis, 50-100 μm below the skin surface. Melanin is a polymer that provides us protection from the sun because of its light absorption properties, and its synthesis is stimulated when skin is exposed to sunlight. Its concentration is variable ranging from very low in light Caucasian skin (type I) to very high in black African skin (type VI). The skin types are mentioned according to the Fitzpatrick Skin-Type Chart. The dark red color of oxygenated hemoglobin circulating through the microvascular network of the dermis (50-500 μm below skin surface) gives a pinkish hue to skin. This can be clearly seen on Caucasian skin because it contains only small amounts of melanin and is therefore nearly transparent, exposing the color of the hemoglobin underneath it.

Carotenes are a large group of molecules usually found in carrots and tomatoes. If we consume carotene-rich products, some carotene molecules accumulate in the epidermis and dermis, while the remaining ones circulate in the blood stream.

Their absorption peak in normal skin is at a wavelength of 482 nm. In order to develop a yellowish tint on account of the carotenes, an individual has to have a high intake of carotenoid rich food. Their color is more intense on hand palms and feet soles, as here the epidermis is much thicker than in the rest of the body, and carotenoids accumulate mostly in the epidermis. In this thesis only the absorption values of hemoglobin are relevant for the blood interference analysis in the autofluorescence spectrum of skin within the visible range.

2.3. Light-Tissue Interaction

Light is composed of photons (light units) and is characterized by frequency and wavelength. Visible light has wavelengths ranging from 400 to 700 nm. The lower range outside of it (100–400 nm) is referred to as ultra violet light (UV), and the range between 700 nm–1000 μm is called infrared (IR). These two regions are not visible for the human eye.

The incident light is swayed and modified by the capacity and inherent structure of the sample (e.g. tissue) to absorb, reflect, transmit or scatter light, as shown in Figure 2.2. Knowing the amount of reflected light and the incident light intensity, the transmittance value can be easily calculated. Since light intensity I[cd] is the perceived power of a source emitting light in a certain direction, its value is wavelength dependent. If a sample has a high reflection intensity, it means that its light absorbance is low. On the other side, direct reflection is the difference in the refractive index a between air and a medium. Owing to this fact, light can be reflected at the surface into a single outgoing direction when tissue is illuminated rather than being diffusely scattered.

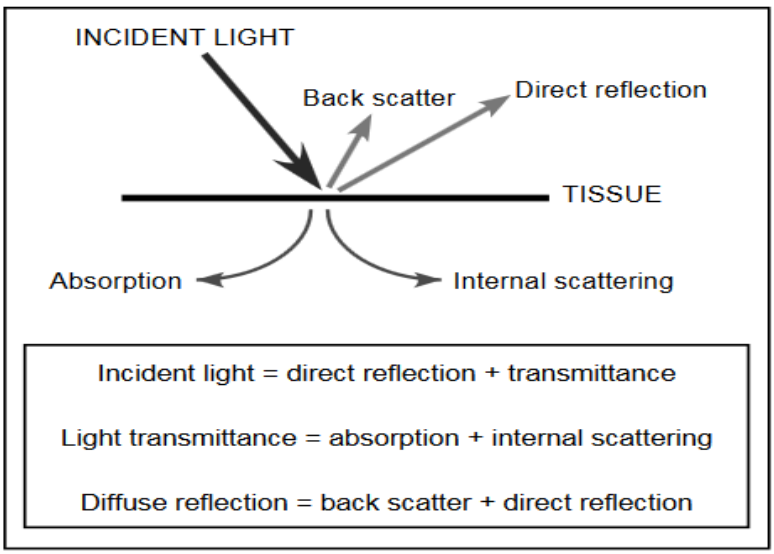

Figure 2.2 Light tissue interaction

The incident light intensity Io decreases exponentially with the molar absorptivity of the absorber in dependence of the wavelength, ε(λ)[ml/(g·mm)], concentration of the absorbers in the material, C[g/ml], and the light travel distance through the material, l[mm]. This proportionality is stated by the Beer–Lambert law, defined in Eq. 2.1. Irepresents the recorded remitted intensity. If I is less than Io, then the sample has ab-sorbed some of the light. However, the Beer–Lambert law is only valid if at least four conditions are fulfilled:

1) light should be monochromatic (one color),
2) the absorbing medium should not scatter light,
3) the incident light should have parallel rays traversing the same length
4) and if two or more absorbers are present their absorption process should be independent.

Despite these limitations, the Beer's law is the basis for spectroscopy measurements

Eq. 2.1 $$I(\lambda) = I_o(\lambda) \cdot e^{-\varepsilon(\lambda) \cdot C \cdot l}$$

The knowledge about the optical properties μa, μs and g of human blood and tissue provide important information for therapeuticand diagnostic applications in laser medicine and medical diagnostics. In addition, they are dependent on physiological parameters like osmolarity, oxygen saturation, hematocrit, flow conditions, etc. During light transmittance two phenomena of scattering or absorption may happen to the photons. Scattering results from a forced change in the light direction, due to the internal structure, differences in refractive index and composition of the tissue (e.g. mitochondria and collagen fibers can scatter light). The scattering coefficient μs [cm^{-1}] describes how many times per unit length a photon will change its direction. In a homogeneous medium free from particles no scattering exists. Eq. 2.2 gives the relationship between scattering coefficient and wavelength, where A and b are constants:

Eq. 2.2 $$\mu_s = A \cdot \lambda^{-b}$$

In contrast, absorption occurs when the light energy is absorbed by molecules in the tissue, for example by hemoglobin. The absorption coefficient μ_a[cm^{-1}] describes the probability per unit distance for an absorption event to occur and is strongly wavelength dependent. In other words, it indicates how easily a medium can be penetrated and takes values between 0 and 1. The higher the absorption coefficient, the smaller the reflection. As denoted in Eq. 2.3, μ_a is the sum of the product of the extinction coefficient ε[$M^{-1}cm^{-1}$] and the concentration c [M] of the absorber. Depending on the molecule, the absorbed energy is partly or completely converted into heat, resulting in a temperature increase in the tissue. In case of fluorophores, part of the absorbed energy is re-emitted in form of fluorescence. Melanins, water, lipids, deoxy- and oxyhemoglobin are the principal absorbers in the human body. Since the overall absorption in tissue is low in the wavelength region 650-1300 nm, this interval is called tissue optical window. When the absorption is low, light can penetrate deep into the tissue.

Eq. 2.3 $$u_a(\lambda) = \sum_k \varepsilon_k(\lambda) \cdot c_k(\lambda)$$

To determine the approximate depth at which light absorption happens, the reversal function of μa is calculated (Eq. 2.4). It indicates the depth which is reached by most of the photons. The energy of the photons is wavelength dependent, so that is why light with large wavelengths (~600 nm) penetrate deeper in tissue than light with shorter wavelengths.

Eq. 2.4 $$d_a = 1/\mu_a$$

The anisotropy factor g describes the amount of forward direction retained after a single scattering event. Anisotropy means that light will not be scattered with the same probabilities in all directions. g is the mean value of cos (θ), where θ is the angle between the incoming light and the scattered light (Eq. 2.5). If the scattering is equal in all directions (isotropic), g is close to zero. A value of g close to one means that the photons are rather scattered in the forward direction, and a value of g = -1 means total backscattering. In tissue g has values between 0.7 and 0.9 and the light is mostly scattered in a forward direction.

Eq. 2.5 $$g = mean(\cos(\theta))$$

If light is scattered many times in tissue, light will become diffuse and μ_s and the g factor cannot be separated. Therefore the reduced scattering coefficient μs' (Eq. 2.6) is used to determine how far the photons must travel before light can be classified as isotropic. Many small steps with a size of $1/\mu_s$'[cm] describe photon movement. Each step has only one partial deflection angle θ. If scattering occurs before absorption, the value of μ_a will be much smaller than μ_s'.

Eq. 2.6 $$\mu_s' = \mu_s(1 - g)$$

The total attenuation coefficient μ_t[cm-1] is the sum of the absorption coefficient μ_a and the scattering coefficient μ_s, thus μ_t describes light transmittance (Eq. 2.7).

Eq. 2.7 $\mu_t = \mu_a + \mu_s$

Diffuse reflection means that the incident light is spread at a number of angles, and it occurs mostly on uneven surfaces. If the reflection is direct (mirror-like, on a high polished flat surface), then the angle of the reflection is the same as the angle of incidence. Backscattering takes place when the light, which entered the tissue initially, goes back to the direction it came from with another angle as a result of scattering in the tissue.

2.4. Fluorescence Spectroscopy

Fluorescence spectroscopy can detect or trace quantities of inorganic, organic, mutagenic, toxic, or carcinogenic fluorophores b from a sample. Besides, spectroscopy is a highly sensitive, safe and quick method. Molecules can vibrate and rotate, causing the energy to split into several sub-levels. If the energy of an incoming photon matches the difference between two energy levels in the molecule, the photon can be absorbed. When the molecule releases excess of energy, heat and/or light emission result. The emitted photons have different frequencies which can be analyzed by a spectrometer. This device measures and records the intensity per frequency, wavenumber or wavelength. The emission spectrum is of a lower energy and a longer wavelength than the absorbed light, due to the previous loss of energy. Hence, the emitted light has a different color as the absorbed light. The fluorescence process can be summarized in 3 steps (see Figure 2.3):

1) **Excitation**: a beam of light stimulates electrons in a fluorophore.
2) **Energy loss**: until the fluorophore loses some energy, it remains in an unstable transient status, adopting the lowest excited state for a very short time.
3) **Emission**: The fluorophore goes back to the ground state. The energy excess is released as light and the substance appears luminous ($\lambda em > \lambda ex$).

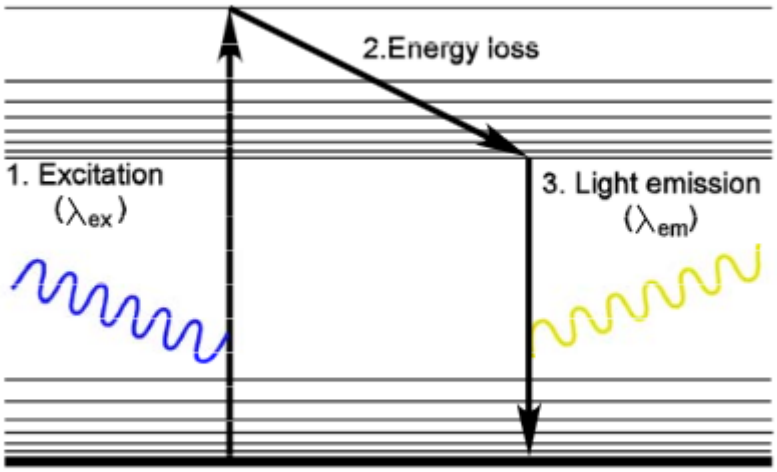

Figure 2.3 Fluorescence process

Almost all fluorophores can undergo the fluorescence process for indefinite times and can thus generate a signal many times. Others turn into instable structures after several illuminations and they can no longer fluoresce. This process is known as photobleaching. Details about it will not be explained in this report.

Fluorescence excitation and emission spectra of fluorophores

As already mentioned before, a fluorophore is a substance capable of emitting light after having absorbed energy. Endogenous fluorophores originate from an organism, tissue or cell, giving rise to autofluorescence. In contrast, exogenous fluorophores have their origin outside the organism and they have to be added to a target molecule in order to obtain fluorescent signals from the molecule, cell or tissue.

Usually, spectroscopic measurements for tissue diagnostics are preformed with a wavelength between the UV and IR spectra. To perform fluorescence spectroscopy on a specific fluorophore, its maximum absorption and emission peak should be considered. Each fluorophore has a specific wavelength at which most of its molecules absorb a maximum of energy. Outside of the energy absorption range, there is no excitation or emission.

Autofluorescence

Autofluorescence is the fluorescence of a tissue due to its endogenous fluorophores. Normally, it occurs upon excitation with blue or UV light. It can help to

recognize the structures of interest (e.g. cancerous tissue from healthy tissue) or it can interfere during detection of other fluorophores. Tissue autofluorescence is usually excited by light in the blue-green region. Most cells contain endogenous fluorophores in their mitochondria and lysosomes. They become excited by UV/blue light of suitable wavelength. The most common fluorophores in the human body are flavin (FAD) and pyridinic (NADH) coenzymes, aromatic amino acids and lipopigments. Normally, the emission spectra of these substances are broad as a result of the interaction between neighboring molecules and the large number of vibration levels. If there is a malignant transformation in the tissue its endogenous fluorophores undergo a change. Also the often increased vascularization in tumors can lead to a lower fluorescence level, since the blood flow can absorb a large amount of light. These modifications can be detected in the intensity and spectral profile of autofluorescence. Examples of endogenous fluorophores in the human skin and brain are listed in Table 2.1.

Table 2.1 Excitation and emission from endogenous fluorophores [15, 16]

Fluorophore	Tissue			$\lambda_{Excitation}$ [nm]	$\lambda_{Emission}$ [nm]
	Skin	Brain	Blood		
NADH	x	x	x	350	460
FAD	x	x	x	410	510-530
Elastin	x	x	-	420, 460, 360, 425	500, 540, 410, 490
Collagen	x	x	-	325, 333, 370	380, 400, 460
Tryptophan	x	x	x	275	350
Endogenous	x	x	x	260, 400	610, 630, 675
Lipopigments	x	x	-	340 – 395	450, 600
Keratin	x	-	-	370	460

Autofluorescence of the skin

Biological tissues, like the skin, have various endogenous fluorophores such as tryptophan (an aromatic amino acid), NAD (nicotinamide adenine dinucleotide) and structural proteins like elastin and collagen. Their optical properties depend on their actual metabolic status and the environment, resulting on modifications in the distribution and amount of the fluorophores. Hence, autofluorescence can provide information about the physiological and morphological state of cells and tissues in some cases without the need of staining or fixing the samples. According to different studies, peaks of excitation and emission were obtained for skin at 380 nm and 470 nm respectively.

Autofluorescence of the blood

According to one study by Masilamani et al., the best blood autofluorescence results are given at an excitation wavelength of 400 nm. Owing to the porphyrin

fluorophores, healthy blood shows two weak peaks at 590 nm and 630 nm (Figure 2.4).

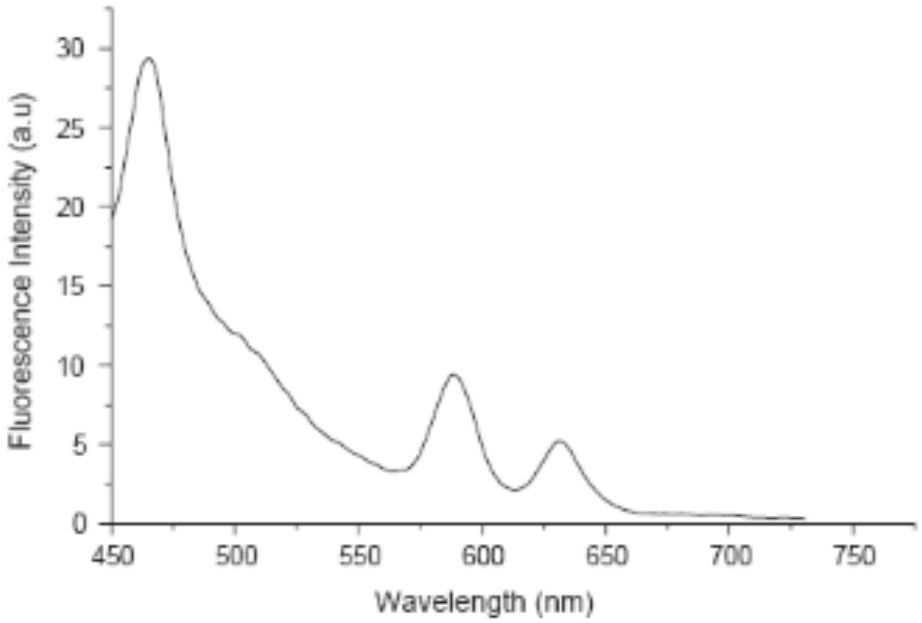

The strong band present at 465 nm is due to acetone and saline water, which were used to extract the blood cells prior to the measurement. A weak band at 495 nm is also observable due to acetone fluorescence. Both bands are seen independent of the instrument parameters for the autofluorescence measurements as well as of the individuals' sex and age. It should be mentioned that the blood autofluorescence spectrum may change in cancer patients by showing peaks due to porphyrin.

3. Devices and Methods

In order to measure fluorescence and absorption 2 devices were used:

1) UV-Vis Perkin Elmer Lambda 95
2) Femtopower Compact Pro Laser

UV-Vis Perkin Elmer Lambda 950

UV-Vis Perkin Elmer Lambda 950 is a spectrometer which in physics is an apparatus to measure a spectrum[1].There are different categories of spectrometers such as:

1) Optical spectrometer: Optical spectrometers (often simply called "spectrometers"), in particular, show the intensity of light as a function of wavelength or of frequency. The deflection is produced either by refraction in a prism or by diffraction in a diffraction grating.

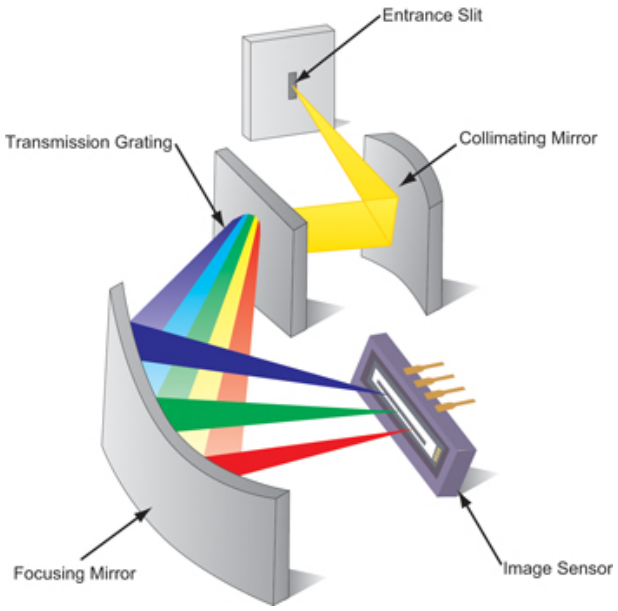

2) Time-of-flight spectrometer: The energy spectrum of particles of known mass can also be measured by determining the time of flight between two detectors (and hence, the velocity) in a time-of-flight spectrometer. Alternatively, if the velocity is known, masses can be determined in a time-of-flight mass spectrometer.

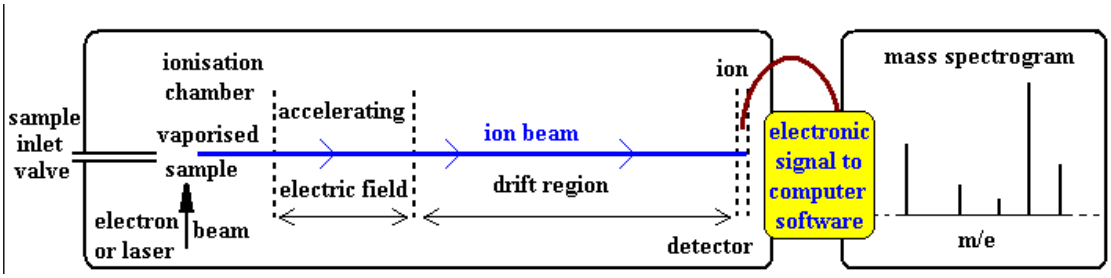

3)Magnetic spectrometer: When a fast charged particle (charge *q*, mass *m*) enters a constant magnetic field *B* at right angles, it is deflected into a circular path of radius *r*, due to the Lorentz force.

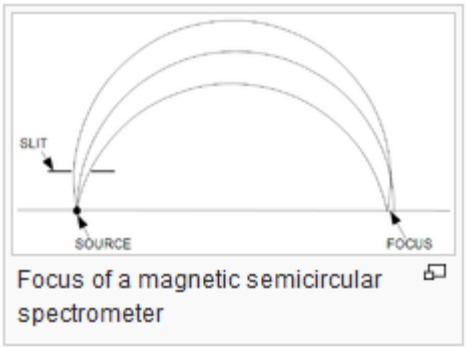

Focus of a magnetic semicircular spectrometer

The momentum *p* of the particle is then given by

$$p = mv = qBr,$$

where *m* and *v* are mass and velocity of the particle. The focussing principle of the oldest and simplest magnetic spectrometer, the semicircular spectrometer, invented by J. K. Danisz, is shown below. A constant magnetic field is perpendicular to the page. Charged particles of momentum *p* that pass the slit are deflected into circular paths of radius $r = p/qB$. It turns out that they all hit the horizontal line at nearly the same place, the focus; here a particle counter should be placed.

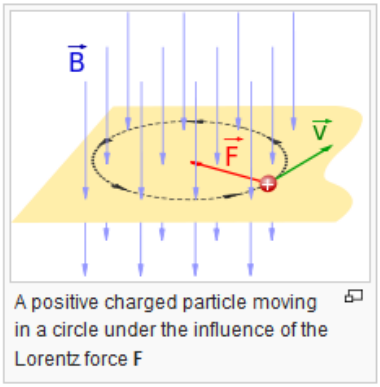

A positive charged particle moving in a circle under the influence of the Lorentz force F

Since Danysz' time, many types of magnetic spectrometers more complicated than the semicircular type have been devised.

4) Mass spectrometer: A mass spectrometer is an analytical instrument that is used to identify the amount and type of chemicals present in a sample by measuring the mass-to-charge ratio and abundance of gas-phase ions.[2]

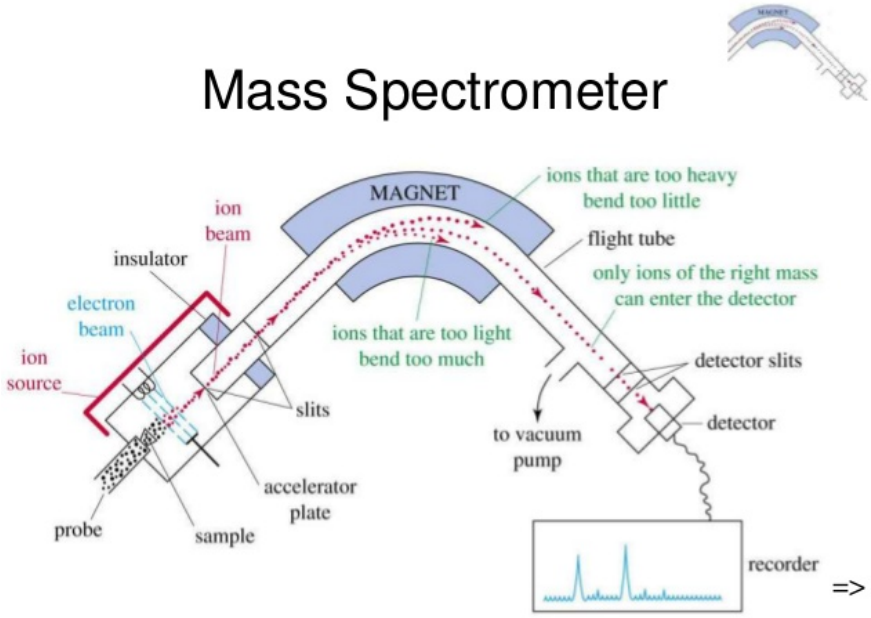

UV-Vis Perkin Elmer Lambda 950 that we used for our expirement is a mass spectrometer that has the ability to measure spectrum from 250nm to 2500nm. The spectrometer features a double-beam, double monochromator, ratio recording optical system.

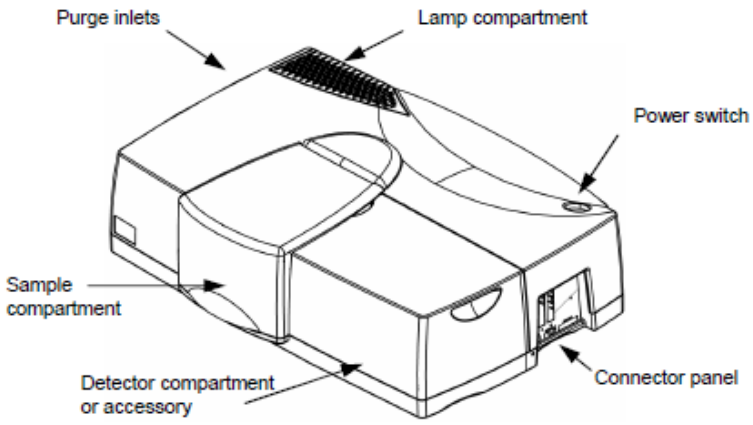

The Lambda 950 Spectrometer features an all-reflecting, double-monochromator optical system. The optical components are coated with silica for durability. Holographic gratings are used in each monochromator for the UV/Vis range and the NIR range.The optical system is depicted schematically in the Figure below.

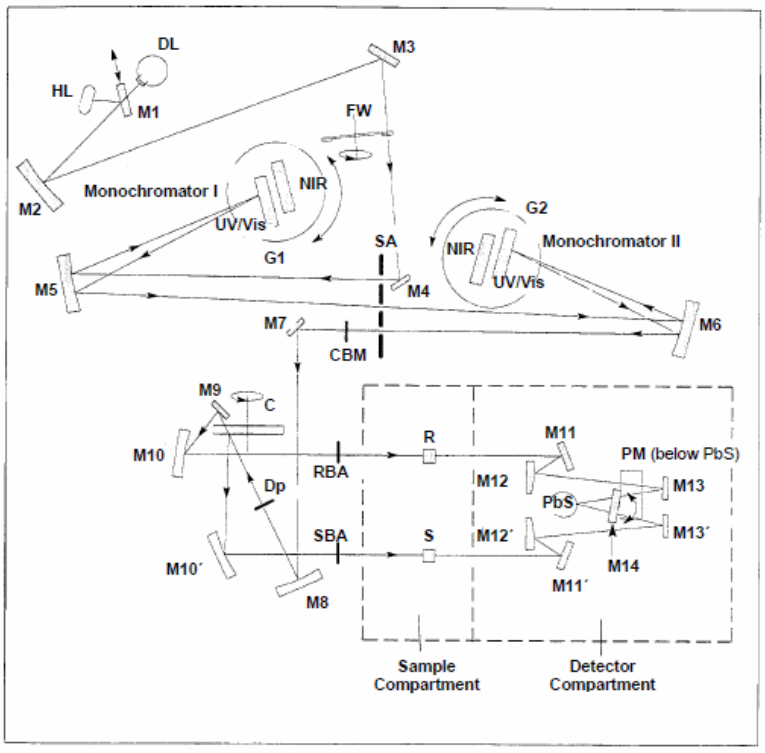

Figure 7 Schematic of Optical System

Two radiation sources, a deuterium lamp (DL) and a halogen lamp (HL), cover the workingwavelength range of the spectrometer.For operation in the near infrared (NIR) and visible (Vis) ranges, source mirror M1 reflects the radiation from

the halogen lamp onto mirror M2. At the same time it blocks the radiationfrom the deuterium lamp.

For operation in the ultraviolet (UV) range, mirror M1 is raised to permit radiation from the deuterium lamp to strike source mirror M2. Source change is automatic during monochromator slewing. Radiation from the respective source lamp is reflected from mirror M2 via mirror M3 throughan optical filter on the filter wheel assembly (FW) to mirror M4.

The filter wheel is driven by a stepping motor to be in synchronization with themonochromators. Depending on the wavelength being produced, the appropriate opticalfilter is located in the beam path to prefilter the radiation before it enters the monochromator. Filter change is automatic during monochromator slewing. From mirror M4 the radiation is reflected through the entrance slit of Monochromator I. All slits are located on the slit assembly (SA). The radiation is collimated at mirror M5 and reflected to the grating table G1. Depending on the current wavelength range, the collimated radiation beam strikes either the UV/Vis grating or the NIR grating (NIR version only).

The radiation is dispersed at the grating to produce a spectrum. The rotational position of the grating effectively selects a segment of the spectrum, reflecting this segment to mirror M5 and then through the exit slit. The exit slit restricts the spectrum segment to a nearmonochromatic radiation beam. Grating change is automatic during monochromator slewing. The exit slit of Monochromator I serves as the entrance slit of Monochromator II. The radiation is reflected via mirror M6 to the appropriate grating on grating table G2 and then back via mirror M6 through the exit slit to Mirror M7. The rotational position of grating table
G2 is synchronized to that of G1. The radiation emerging from the exit slit exhibits high spectral purity with an extremely low stray radiation content.

In the UV/Vis and NIR range a choice is provided between a fixed slit width, a servo slit, and a slit program. When the servo slit is selected, the slit widths change automatically during scanning to maintain constant energy at the detector. From mirror M7 the radiation beam is reflected via toroid mirror M8 to the chopper assembly (C). As the chopper rotates, a mirror segment, a window segment and two dark segments are brought alternately into the radiation beam. When a window segment enters the beam, radiation passes through to mirror M9 and is then reflected via mirror M10 to create the reference beam (R).

When a mirror segment enters the beam the radiation is reflected via mirror M10´ to form the sample beam (S). When a dark segment is in the beam path, no radiation reaches the detector, permitting the detector to create the dark signal. The radiation passing alternately through the sample and reference beams is reflected by mirrors M11, M12, M13, and M11´, M12´, M13´, respectively of the optics in the detector assembly onto the appropriate detector.

Mirror M14 is rotated to select the required detector. A photomultiplier (PM) is used in the UV/Vis range while a lead sulfide (PbS) detector is used in the NIR range. Detector change is automatic during monochromator slewing. At the cell plane, each radiation beam is approximately 12 mm high. The width of the radiation beams is dependent on the slit width. At a slit width of 5 nm each radiation beam isapproximately 4.5 mm wide.

To permit minimum sample volumes to be measured in micro cells, the height of the radiation beam must be reduced in the active cell area. A common beam mask (CBM) is mounted between the slit assembly (SA) and mirror M7. This mask restricts the cross-section of both the sample beam and the reference beam in the respective

cell area. The radiation beam can be reduced from the maximum height of 11.7 mm to 0.0 mm in 50 steps. During all scanning operations, the monochromators stop slewing while a filter, source, or detector change is in progress.

Femtopower Compact Pro Laser

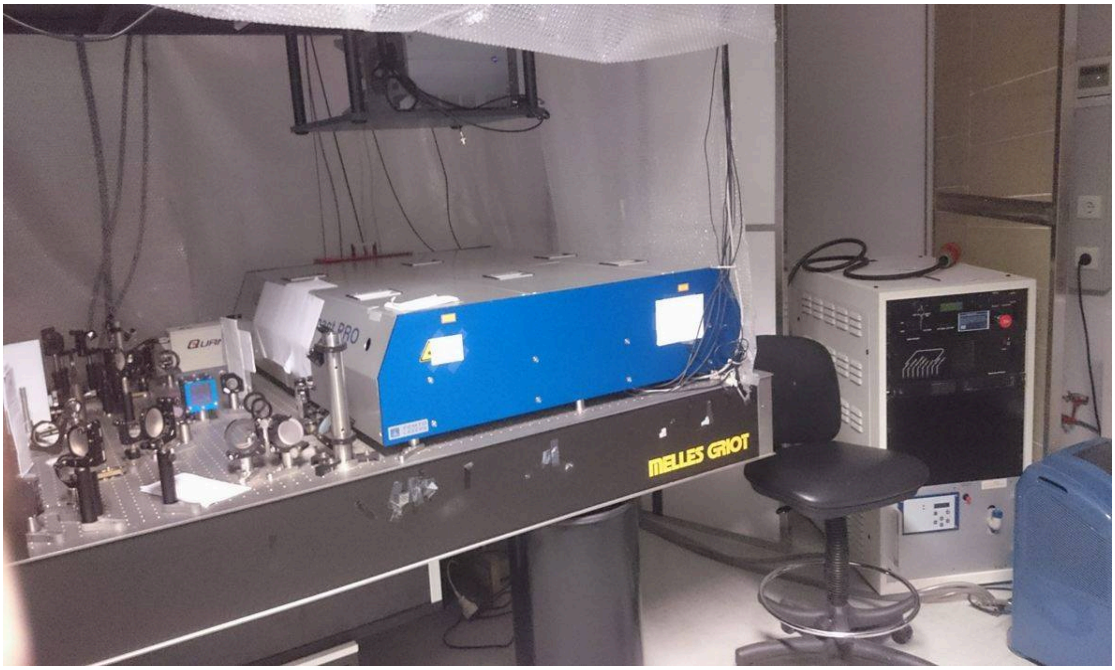

The FEMTOPOWER™ COMPACT™ PRO is a kHz-repetition rate, multi-pass titanium-sapphire amplifier which is seeded by broadband femtosecond pulses from a mirror-dispersion controlled titanium-sapphire oscillator and uses a modified version of the chirped-pulse-amplification scheme. The FEMTOPOWER™ COMPACT™ PRO consists of the main system assembly (incorporating the oscillator, the pulse stretcher, the amplifier and the pulse compressor), an external Amplifier Control Unit, an external Remote Control Unit (FDA-version only), an external vacuum pump, an external chiller/cooler, and an external Pockels cell driver with Trigger Generator. The FEMTOPOWER™ COMPACT™ PRO requires two laser energy sources for operation:

1. A cw, frequency-doubled Nd:YVO_4 laser for pumping the oscillator. Space is provided so that the oscillator pump laser head can be mounted inside the FEMTOPOWER™ COMPACT™ PRO's protective housing.

2. a kHz-repetition rate, Q-switched, frequency-doubled Nd:YAG or Nd:YLF laser for pumping the amplifier.

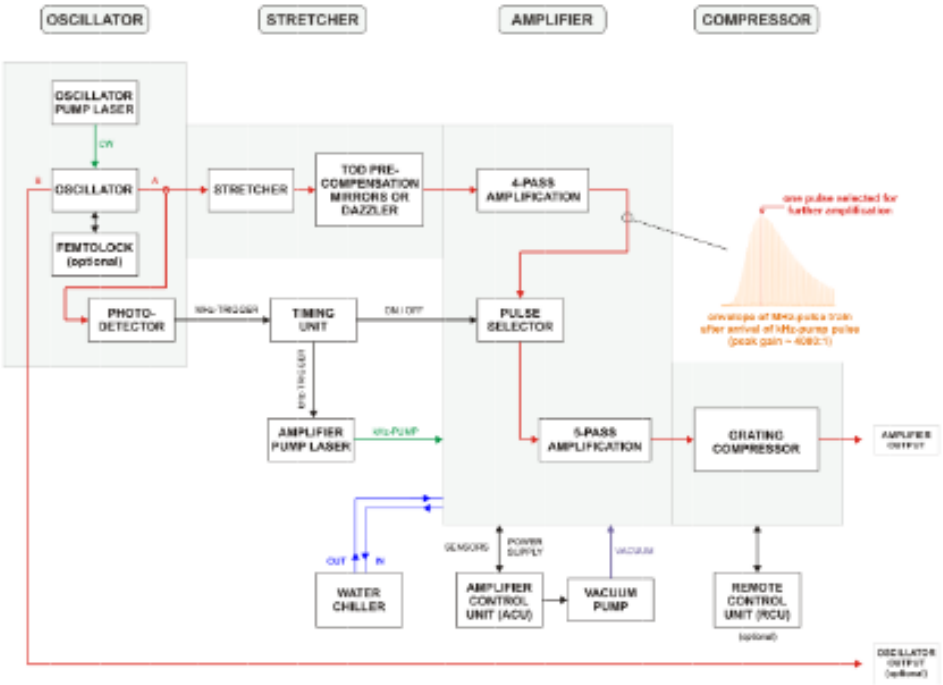

Fig. 1: Illustrates the basic operation principle of the FEMTOPOWER™ COMPACT™ PRO system

A mirror-dispersion controlled oscillator generates broadband (>100 nm), ultrashort (~10 fsec) pulses at ~76MHz repetition rate. The pulses are stretched to a safe value for amplification by traversing a suitable amount of optical glass. Third-order dispersion pre-compensation is achieved by a certain number of reflections from TOD-dispersion compensating mirrors. The pulses are then amplified by multiple passes through a kHz-pumped amplifier assembly to ~ 1 mJ. After the first four passes a single pulse is selected from the MHz-pulse train to be further amplified in another five passes. After amplification the pulses are recompressed to less than 30 fsec by a prism compressor.

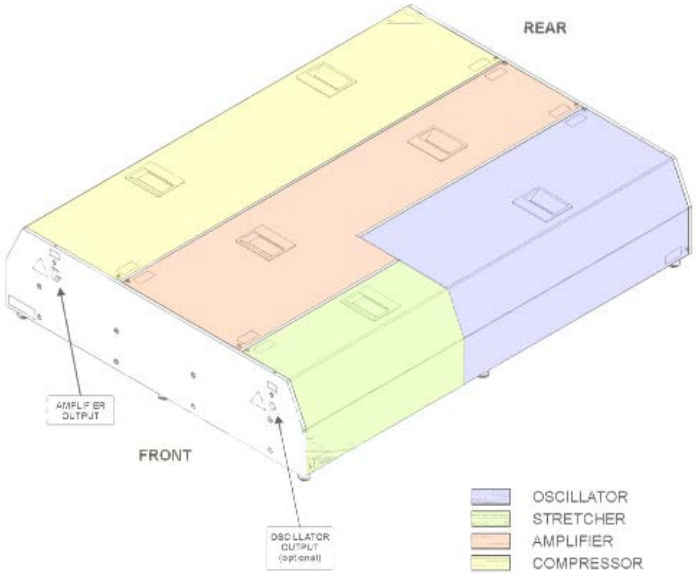

Fig. 2: FEMTOPOWER™ COMPACT™ PRO functional overview

The beam follows the path below to reach our tissue:

1) Stretcher section: The seed beam from the oscillator entering the stretcher section (via perisope OOP1) has a beam height of 2" and is horizontally polarized. The beam passes through a Faraday isolator FI that prevents back-reflections from the amplifier disturbing the oscillator. At the output of the Faraday isolator the beam height is 2.25" and its polarization has been changed to vertical. The beam then makes a number of reflections on two pairs of TOD-precompensating mirrors TOD1/2 and TOD/3/4 and passes through the main stretcher PS1, a Brewster-angled block of SF57 glass, is retroreflected back by AP1(that changes the beam height from 2.25" to 2") and makes a second pass through PS1 before being picked off by mirror APM1. The seed beam is then reflected by mirror ASM1 and is sent into the amplifier section by turning mirror APM3. The beam height at this point is 2" and the beam polarization vertical. The leakage through mirror ASM1 is directed onto the photodetector PD1via turning mirror APM2. The signal from this photodetector is fed to the Triggerbox and serves as the master clock for all timing signals, i.e. the trigger signals for the pump laser, the Pockels cell on/off, the XPS reference and the APS spectrometer are derived from this signal by proper division and adjustable delays.

2) Amplifier section: The beam entering the amplifier section is changed in both height (from 2" to 66mm) and polarization (from vertical to horizontal) by periscope AP2 and is directed into the amplifier by turning mirrors APM4 and APM5. The multipass amplifier is comprised of the focussing mirrors AFM1 and AFM2, the gain medium (a TEC-cooled titanium-sapphire crystal mounted in a vacuum chamber to prevent condensation), and two pairs of retroreflectors ARR1A/B and ARR2A/B. On each pass through the gain medium these retroreflectors shift the beam horizontally

for the next pass. The beam path through the multipass amplifier is defined by aperturesAHM1 and AHM2, that serve to reduce amplified spontaneous emission. Amplification takes place in two parts.

The first four passes are made by the full MHz pulse train. By inserting the auxiliary mirror AAM1 the second pass or the fourth pass can be directed onto photodetector PD3via beamsplitter ABS2for alignment purposes and for checking the amplification factor.

After the fourth pass the beam is picked off by mirror APM6, passes through polarizer APBS1and then the Pockels cell PCwhich selects a single pulse out of the MHz pulse train (at 1 kHz repetition rate) near the maximum of the gain curve. At the Pockels cell output the pulses in the MHz pulse train are all horizontally polarized (PCoff) except the one pulse that is selected for further amplification (PCon, for about 10 nsec), which is vertically polarized. The half-wave voltageof the Pockels cellis about 6.3 kV. The periscope AP3changes both the beam heigth (from 66mm to 61mm) and the polarization of the pulses exiting the Pockels cell. At the polarizer APBS2all the pulses where the Pockels cell is off are therefore rejected and only the one pulse where the Pockels cell is on is transmitted and further amplified. The Berek compensator BC(a variable waveplate where both the retardation and the orientation can be adjusted) allows to optimize the pre-pulse contrast. After the pulsehas made another four passes through the gain medium (passes 5thto 8th) it is picked off by mirrors APM9 / AM10, passes through the mode-matching lens AL1(which serves to mode-match the beam size in the crystal for the final pass) and is sent back by mirrors APM11, APM12at a beam height of 74 mm. After the 9thpass the beam is picked off by mirror APM13 and is directed into the prism compressor section. A small part (< 0.5%) of this amplifier output beam is split off by beam splitter CBS1and directed onto photodetector PD3via turning mirror AMM1. Three neutral density filters (ND10, ND30– corresponding to 10:1 and 1000:1) mounted in flip-up holders allow to attenuate the beam such that PD3is not saturated. The signal on photodetector PD3can be used to monitor system performance (e.g. pulse-to-pulse jitter) and to optimize the pre-pulse contrast.

3)Compressor section: The amplified beam entering the compressor section passes over turning mirrors CSM1, CSM2 and CSM3and through telescope CTL1/2 (that increases the beam diameter and collimates the beam) before entering the prism compressor via turning mirror CSM4. The compressor consists of the two Brewster-prism pairs CPR1A/B, CPR2A/B and four folding mirrors CFM1 to CFM4. The spatially dispersed beam after CPR2B is retroreflected back by mirror CSM5, makes a second pass through the prism pairs CPR1A/B, CPR2A/B (vertically offset), is reflected by mirror CSM6and is emitted from the amplifier output aperture. The second prism pair CPR2A/Bis mounted on a translation stage that allows to adjust the dispersion of the prism compressor and to optimize the pulse duration at the output. The beam path through the prism compressor is set by three iris diaphrams (A1, A2 and A3).

4)Amplifier pump laser beam path: The amplifer pump beam enters the housing via periscope PP1and is focused into the amplifier crystal by lens PL1 (mounted on a translation stage). The pump beam notabsorbed in the first pass is transmitted by mirror AFM1and re-focused into the crystal by focussing mirror APFM1 (also mounted on a translation stage). Dependingon the characteristics of the pump beamsome additional beam-shaping optics may be necessary, typically a spherical telesope PTL1, PTL2 to achieve the correct beam diameter in the amplifier crystal. If the pump beam is elliptical an additional cylindrical telescope PZTL1, PZTL2 may be required. In some systems a half-wave plate / polarizer combination HWP, TFP allows to adjust the pump power without changing the beam characteristics (as would typically be the case when changing the pump current).

FEMTOPOWER™ COMPACT™	PRO HE
Output	amplifier
Pulse duration (FWHM)	< 30 fs
Spectral width (FWHM) @ 800nm	> 40 nm
Output energy	> 0.8 mJ
Pulse repetition rate	1kHz +/- 5%
Beam diameter ($1/e^2$)	15 mm (nominal)
B-integral of amplified pulses	< 1
Spatial mode	TEM_{00} ($M^2 < 2$)
Contrast ratio	$> 10^7 : 1$ [1] / $> 10^4 : 1$ [2]
Polarization	linear, horizontal
Pulse-to-pulse energy stability	< 1.5 % rms
Beam divergence	< 3 mrad
Pump-laser requirements	Please ask about approved lasers

Tab 1:FEMTOPOWER™ COMPACT™ PRO system specifications

4. Samples

For our expirement we used human's and animal's tissues and we compared the pathological with the healthy in order to detect differences as far as absorption and fluorescence is concerned. The different tissues are listed below:

1)Skin: Skin is the soft outer covering of vertebrates and it is composed of:

- Epidermis
- Basement membrane
- Dermis
- Papillary region
- Hypodermis

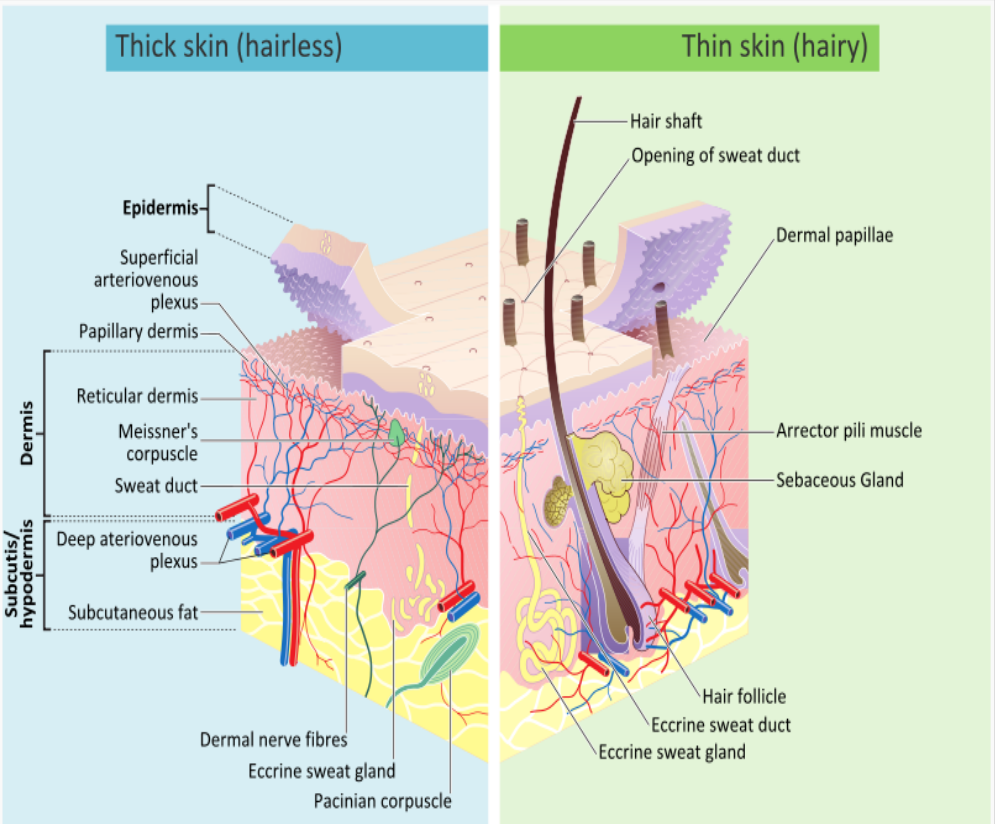

Skin layers, of both the hairy and hairless skin

2) Squamous cell carcinoma: Squamous cell carcinoma or squamous cell cancer (SCC or SqCC) is a cancer of a kind of epithelial cell, the squamous cell and the second-most common cancer of the skin (after basal-cell carcinoma but more common than melanoma). These cells are the main part of the epidermis of the skin, and this cancer is one of the major forms of skin cancer. However, squamous cells also occur in the lining of the digestive tract, lungs, and other areas of the body, and SCC occurs as a form of cancer in diverse tissues, including the lips, mouth, esophagus, urinary bladder, prostate, lung, vagina, and cervix, among others. Despite sharing the name *squamous cell carcinoma*, the SCCs of different body sites can show tremendous differences in their presenting symptoms, natural history, prognosis, and response to treatment.

3) Pilonidal cyst: Pilonidal cyst, also referred to as a pilonidal abscess, pilonidal sinus or sacrococcygeal fistula, is a cyst or abscess near or on the natal cleft of the buttocks that often contains hair and skin debris. Pilonidal cysts are often very painful, and typically occur between the ages of 15 and 35. Although usually found near the coccyx, the condition can also affect the navel, armpit or genital region, though these locations are much rarer.

4)Nevus: Nevus, also known as a mole, is the medical term for sharply circumscribed and chronic lesions of the skin or mucosa. These lesions are commonly named birthmarks or beauty marks. Nevi are benign by definition. However, 25% of malignant melanomas (a skin cancer) arise from pre-existing nevi. Using the term nevus and nevi loosely, most physicians and dermatologists are actually referring to a variant of nevus called the "melanocytic nevus", which are composed of melanocytes. Histologically, melanocytic nevi are distinguished from lentigines (also a type of benign pigmented macule) by the presence of nests of melanocytes, which lentigines (plural form of lentigo) lack.

5)Cornea: The cornea is the transparent front part of the eye that covers the iris, pupil, and anterior chamber.[3] The cornea, with the anterior chamber and lens, refracts light, with the cornea accounting for approximately two-thirds of the eye's total optical power.[4] In humans, the refractive power of the cornea is approximately 43 dioptres.[5] While the cornea contributes most of the eye's focusing power, its focus is fixed. The curvature of the lens, on the other hand, can be adjusted to "tune" the focus depending upon the object's distance. Medical terms related to the cornea often start with the prefix "*kerat*-" from the Greek word κέρας, *horn*.

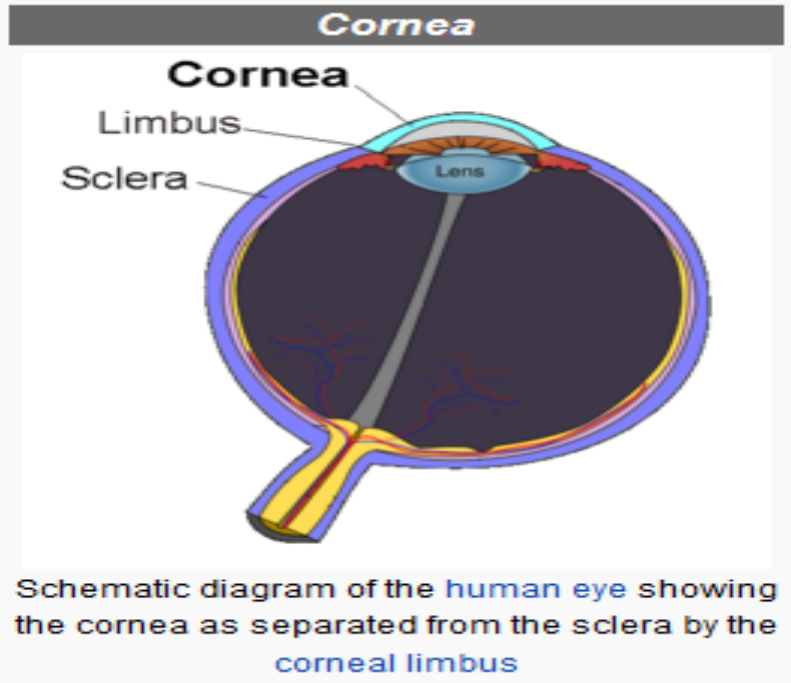

Schematic diagram of the human eye showing the cornea as separated from the sclera by the corneal limbus

The cornea has unmyelinated nerve endings sensitive to touch, temperature and chemicals. A touch of the cornea causes an involuntary reflex to close the eyelid. Because transparency is of prime importance the cornea does not have blood vessels; it receives nutrients via diffusion from the tear fluid through the outside surface and the aqueous humour through the inside surface, and also from neurotrophins supplied by nerve fibres that innervate it. In humans, the cornea has a diameter of about 11.5 mm and a thickness of 0.5–0.6 mm in the center and 0.6–0.8 mm at the periphery. Transparency, avascularity, the presence of immature resident immune cells, and immunologic privilege makes the cornea a very special tissue. The cornea has no blood supply; it gets oxygen directly through the air. Oxygen first dissolves in the tears and then diffuses throughout the cornea to keep it healthy.[6] It borders with the sclera by the corneal limbus. The most abundant soluble protein in mammalian cornea is albumin.[7] In lampreys, the cornea is solely an extension of the sclera, and is separate from the skin above it, but in more advanced vertebrates it is always fused with the skin to form a single structure, albeit one composed of multiple layers. In fish, and aquatic vertebrates in general, the cornea plays no role in focusing light, since it has virtually the same refractive index as water.[8] The human cornea has five (possibly six) layers which from the anterior to posterior are:

1. Corneal epithelium
2. Bowman's layer
3. Corneal stroma
4. Descemet's membrane
5. Corneal endothelium

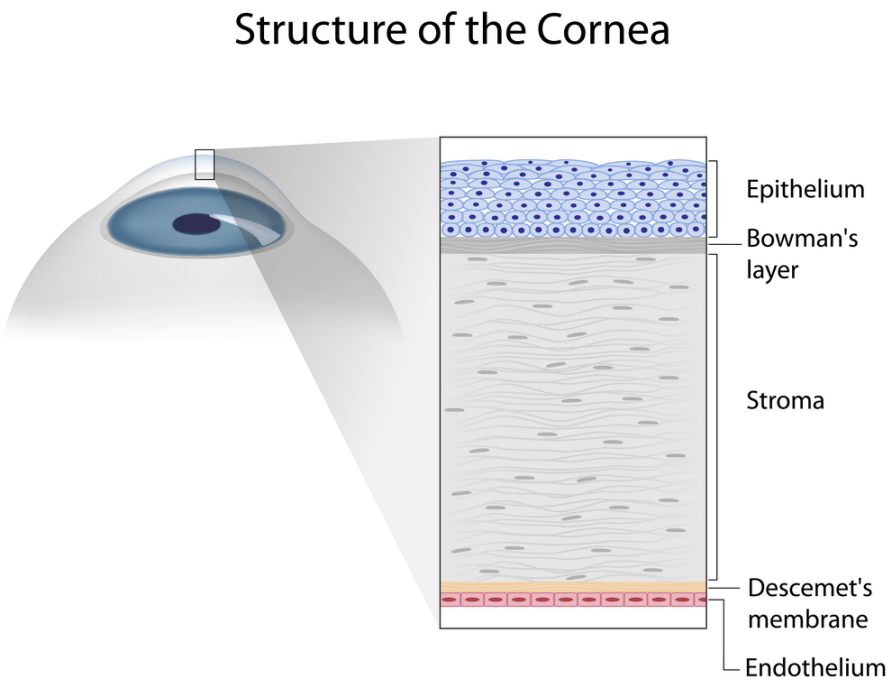

6) Sclera: The sclera,[9] also known as the white of the eye, is the opaque, fibrous, protective, outer layer of the eye containing collagen and elastic fiber.[10] In humans, the whole sclera is white, contrasting with the coloured iris, but in other mammals the visible part of the sclera matches the colour of the iris, so the white part does not normally show. In the development of the embryo, the sclera is derived from the neural crest.[11] In children, it is thinner and shows some of the underlying pigment, appearing slightly blue. In the elderly, fatty deposits on the sclera can make it appear slightly yellow.The human eye is relatively rare for having an iris that is small enough for its position to be plainly visible against the sclera. This makes it easier for one individual to infer where another individual is looking, and the cooperative eye hypothesis suggests this has evolved as a method of nonverbal communication.

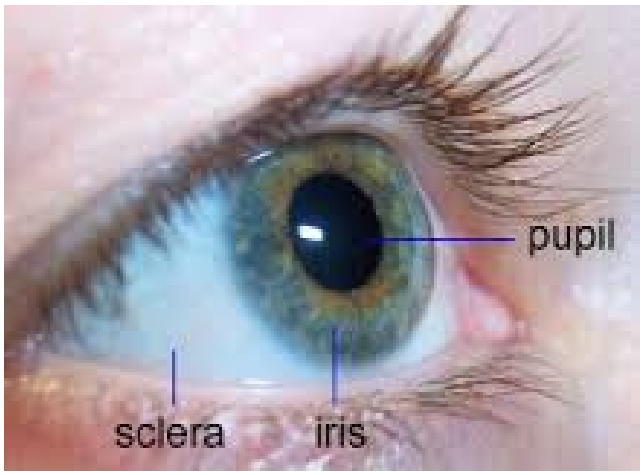

The sclera forms the posterior five-sixths of the connective tissue coat of the globe. It is continuous with the dura mater and the cornea, and maintains the shape of the globe, offering resistance to internal and external forces, and provides an attachment for the extraocular muscle insertions. The sclera is perforated by many nerves and vessels passing through the posterior scleral foramen, the hole that is formed by the optic nerve. At the optic disc the outer two-thirds of the sclera continues with the dura mater (outer coat of the brain) via the dural sheath of the optic nerve. The inner third joins with some choroidal tissue to form a plate (lamina cribrosa) across the optic nerve with perforations through which the optic fibers (fasciculi) pass. The thickness of the sclera varies from 1mm at the posterior pole to 0.3 mm just behind the rectus muscle insertions. The sclera's blood vessels are mainly on the surface. Along with the vessels of the conjunctiva (which is a thin layer covering the sclera), those in the episclera render the inflamed eye bright red.[12]

In many vertebrates, the sclera is reinforced with plates of cartilage or bone, together forming a circular structure called the sclerotic ring. In primitive fish, this ring consists of four plates, but the number is lower in many living ray-finned fishes, and much higher in lobe-finned fishes, various reptiles, and birds. The ring has disappeared in many groups, including living amphibians, some reptiles and fish, and all mammals.[13] The eyes of all non-human primates are dark with small, barely visible sclera.

The collagen of the sclera is continuous with the cornea. From outer to innermost, the four layers of the sclera are:

1. episclera
2. stroma
3. lamina fusca
4. endothelium

7)Pterygium: Pterygium most often refers to a benign growth of the conjunctiva. A pterygium commonly grows from the nasal side of the conjunctiva. It is usually present in the palpebral fissure. It is associated with and thought to be caused by ultraviolet-light exposure (e.g., sunlight), low humidity, and dust. The predominance of pterygis on the nasal side is possibly a result of the sun's rays passing laterally through the cornea, where it undergoes refraction and becomes focused on the limbic area. Sunlight passes unobstructed from the lateral side of the eye, focusing on the medial limbus after passing through the cornea. On the contralateral (medial) side, however, the shadow of the nose medially reduces the intensity of sunlight focused on the lateral/temporal limbus. Symptoms of pterygium include persistent redness from smoke,[14] inflammation,[16] foreign body sensation, tearing, dry and itchy eyes. In advanced cases the pterygium can affect vision[15] as it invades the cornea with the potential of obscuring the optical center of the cornea and inducing astigmatism and corneal scarring.[16] Many patients do complain of the cosmetic appearance of the eye either with some of the symptoms above or as their major complaint. [17]

Pterygium in the conjunctiva is characterized by elastotic degeneration of collagen (actinic elastosis[18]) and fibrovascular proliferation. It has an advancing portion called the head of the pterygium, which is connected to the main body of the pterygium by the neck. Sometimes a line of iron deposition can be seen adjacent to the head of the pterygium called *Stocker's line*. The location of the line can give an indication of the pattern of growth. The exact cause is unknown, but it is associated with excessive exposure to wind, sunlight, or sand. Therefore, it is more likely to occur in populations that inhabit the areas near the equator, as well as windy locations. In addition, pterygia are twice as likely to occur in men than women. Some research also suggests a genetic predisposition due to an expression of vimentin, which indicates cellular migration by the keratoblasts embryological development, which are the cells that give rise to the layers of the cornea. Supporting this fact is the congenital pterygium, in which pterygium is seen in infants.[19] These cells also exhibit an increased P53 expression likely due to a deficit in the tumor suppressor gene. These indications give the impression of a migrating limbus because the cellular origin of the pterygium is actually initiated by the limbal epithelium.[20]

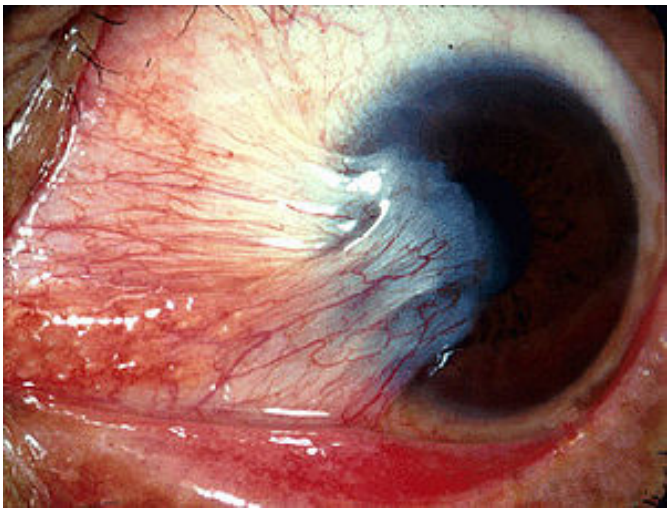

8) Decubitus Ulcers: Decubitus ulcers, also known as pressure sores, bedsores and pressure ulcers, are localized injuries to the skin and/or underlying tissue that usually occur over a bony prominence as a result of pressure, or pressure in combination with shear and/or friction. The most common sites are the skin overlying the sacrum, coccyx, heels or the hips, but other sites such as the elbows, knees, ankles, back of shoulders, or the back of the cranium can be affected. Pressure ulcers occur due to pressure applied to soft tissue resulting in completely or partially obstructed blood flow to the soft tissue. Shear is also a cause, as it can pull on blood vessels that feed the skin. Pressure ulcers most commonly develop in individuals who are not moving about, such as those being bedridden or confined to a wheelchair. It is widely believed that other factors can influence the tolerance of skin for pressure and shear, thereby increasing the risk of pressure ulcer development. These factors are protein-calorie malnutrition, microclimate (skin wetness caused by sweating or incontinence), diseases that reduce blood flow to the skin, such as arteriosclerosis, or diseases that reduce the sensation in the skin, such as paralysis or neuropathy. The healing of pressure ulcers may be slowed by the age of the person, medical conditions (such as arteriosclerosis, diabetes or infection), smoking or medications such as anti-inflammatory drugs.Although often prevented and treatable if detected early, pressure ulcers can be very difficult to prevent in critically ill people, frail elders, wheelchair users (especially where spinal injury is involved) and terminally ill individuals. Primary prevention is to redistribute pressure by regularly turning the person. The benefit of turning to avoid further sores is well documented since at least the 19th century. In addition to turning and re-positioning the person in the bed or wheelchair, eating a balanced diet with adequate protein and keeping the skin free from exposure to urine and stool is very important.The rate of pressure ulcers in hospital settings is high, but improvements are being made. They resulted in 29,000 documented deaths globally in 2013, up from 14,000 deaths in 1990.[21]

5.Expiremental results and discussion

5.1.Absorption

Squamous Cell Carcinoma

Optical absorption measurements, as analyzed previously, are a unique method to investigate the optical properties of the tissues under study. A typical absorption measurement of Squamous cell carcinoma is shown in Figure 5.1. 1. In the y-axis the intensity of transmission is shown, while in the x-axis the wavelength is shown.

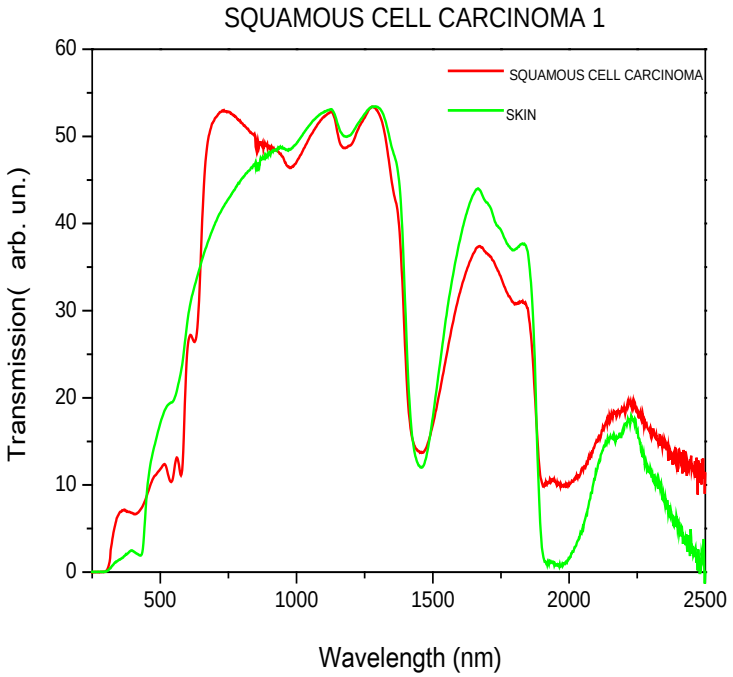

Figure 5.1. 1: Transmission of light as a function of wavelength obtained from squamous cell carcinoma 1

The figure above shows transmission spectra from a squamous cell carcinoma that has been surgically extracted from a seventy six year old man. The carcinoma has been afterwards histologicaly confirmed. In addition to this, the transmission spectrum of healthy skin surgically extracted from a region near the carcinoma is also shown in Figure 5.1. 1 for comparison purposes. It is noteworthy that the shape of the Transmission spectra is different for the two samples. More specifically, at 630 nm to 750 nm the carcinoma's transmission spectrum a rapid ascent with increasing wavelength is observed compared to the transmission spectrum of the healthy skin. Furthermore, it can be seen that from 400 nm to 600 nm the transmission spectrum of

healthy skin exhibits a monotonic rise in the transmission. On the other hand, the transmission spectrum of squamous cell carcinoma shows a more complex behavior. In addition to this, significant spectral differences can be observed in the region from 1000 nm to 1150 nm indicating that the transmission spectra are distinguishable not only at the visible but also at the near infrared wavelength regime. The spectral differences point out a novel spectroscopic method completely different than the histological examination which can detect differences in the response between healthy tissue and carcinoma and is therefore a promising alternative diagnostic method.

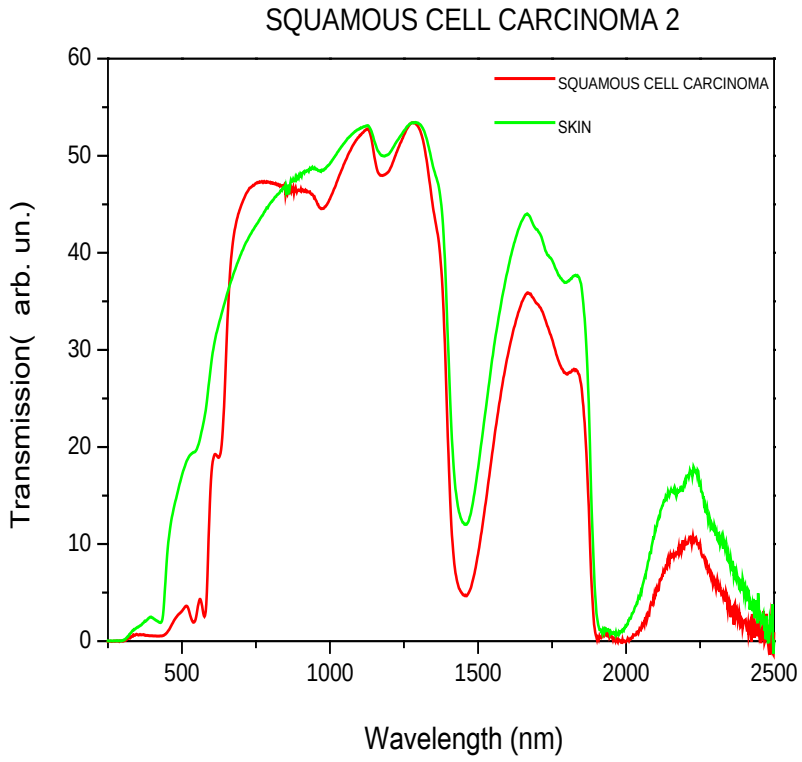

Figure 5.1. 2: Transmission of light as a function of wavelength obtained from squamous cell carcinoma 2

Afterwards another squamous cell carcinoma which was surgically extracted from an eighty one year old man has been measured. This sample was proven to be a squamous cell carcinoma from the histological examination. Similarly to the previous case, and in addition to the malignant tissue, healthy skin from a nearby region has also been surgically extracted and measured in transmission spectroscopy for comparison purposes. The results from the transmission measurements can be seen in Figure 5.1. 2. By a quick inspection of Figure 5.1. 2 we find that it has a lot of similarities with Figure 5.1. 1. More specifically, from 400 nm to 600 nm it can be seen that the carcinoma's transmission spectrum presents a complex behavior with

ascents and descents. On the other hand, the healthy skin's transmission spectrum exhibits a monotonic rise. What is more, in this different case of squamous carcinoma 2 we can detect in the near infrared region of the spectrum the same behavior with squamous cell carcinoma 1. At the region from 1000 nm to 1150 nm the transmission spectrum of both carcinomata show a decline while on the other hand, the spectrum of healthy skin exhibits an augmentation. Additionally, in the wavelength region from 640 nm to 750 nm the carcinoma's spectrum presents a sharp increase in the transmission in contrast to that of healthy skin.

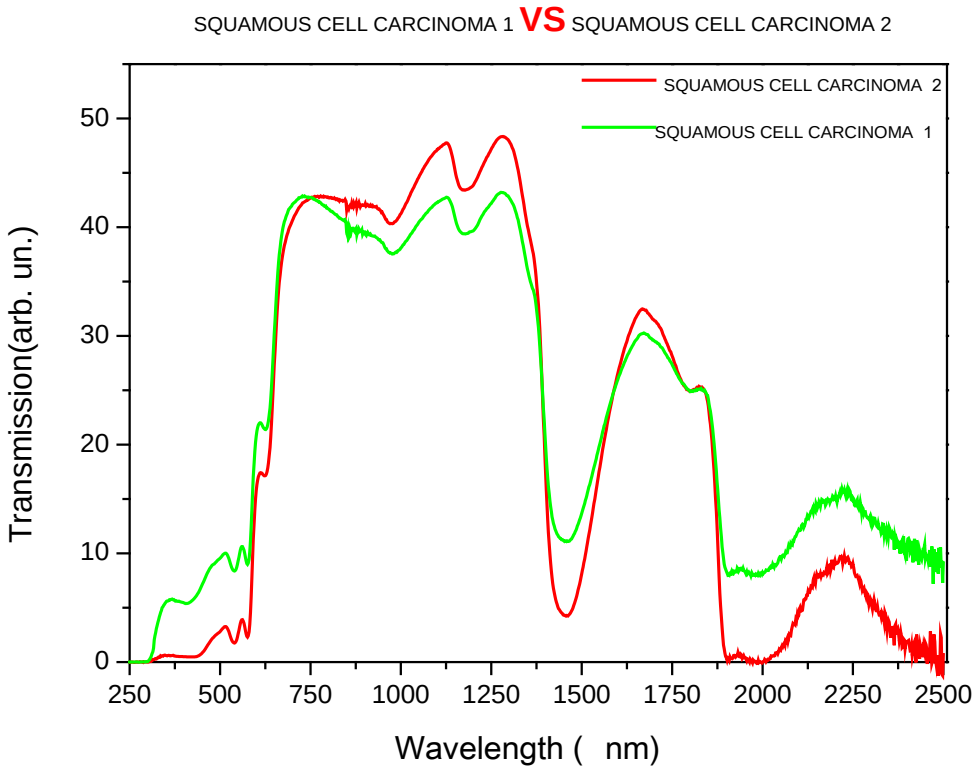

Figure 5.1. 3: Transmission of light as a function of wavelength of obtained from squamous cell carcinoma 1 and 2

To sum up at Figure 5.1. 3 a comparison between the transmission spectra for the two squamous cell carcinomata is presented. By comparison of the two graphs it can be realized that spectral shapes are very similar. Slight intensity variations between the two spectra are attributed to differences in the thickness and other morphological differences that have been most probably introduced during surgical extraction due to imperfect cuts of the tissues and also due to possible differences in the handling of the two different samples during the spectral measurements. Nevertheless, the comparison of the transmission spectra of the two tissues shows

strong similarities and thus constitute a strong evidence that the absorption spectroscopy method is a reliable and powerful diagnostic tool in the determination and distinction between malignant and healthy tissue which arises from the fact that carcinoma and healthy tissue exhibit systematic and characteristic differences in certain regions of their transmission spectra when exposed to illumination by visible and near visible optical wavelengths.

Decubitus Ulcers

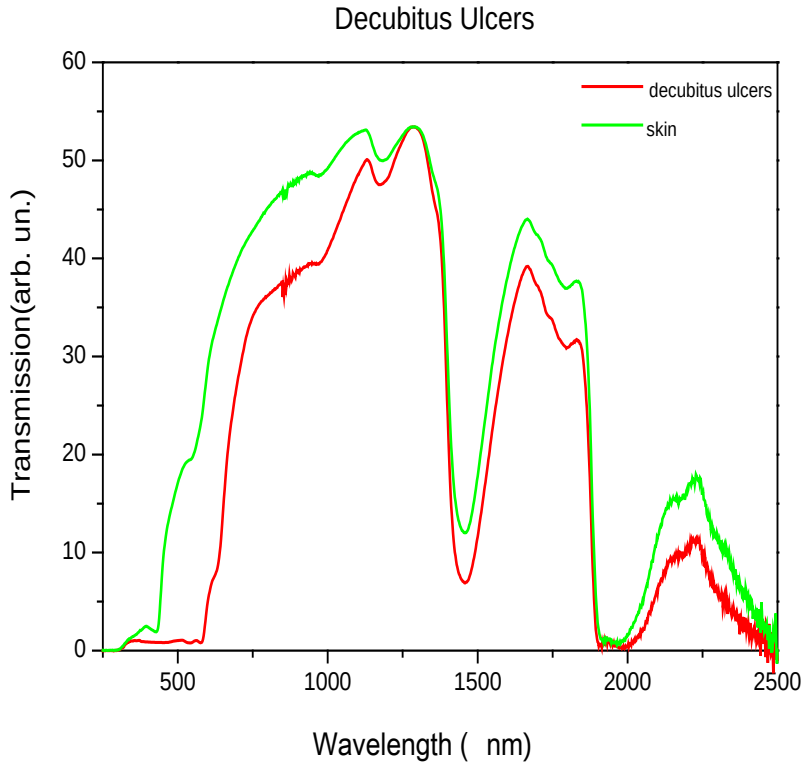

Figure 5.1. 4: Transmission of light as a function of wavelength obtained from Decubitus ulcers

At the next step of our experiment the transmission of light as a function of wavelength obtained from decubitus ulcers has been examined. The specimens were surgically extracted from a ninety two year old woman. In addition to this, healthy skin from a nearby region has also been surgically extracted for comparison purposes. It is obvious at Figure 5.1. 4 that decubitus ulcer's transmission spectrum shows that in the region from 300 nm to 650 nm no light is practically transmitted and this is attributed to high absorption in this specific wavelength region. On the other hand, the

transmission spectrum obtained for healthy skin exhibits a steady rise in the same spectral region. This may be attributed to the total dark color of decubitus ulcers, i.e. very high optical absorption. But the significant finding of this measurement is that differences may extend even at the area of ultraviolet apart from visible and infrared light which had been shown so far (see Figure 5.1. 1 and Figure 5.1. 2). What is more, in this case that dead skin (non cancerous tissue) was measured it has been realized that there are no differences at visible and infrared light that existed at the measurement of absorption of squamous cell carcinomas. Consequently, this is one more indication that cancerous cells have this special correspondence at the measurement of absorption that was previously mentioned.

Pilonidal Cyst

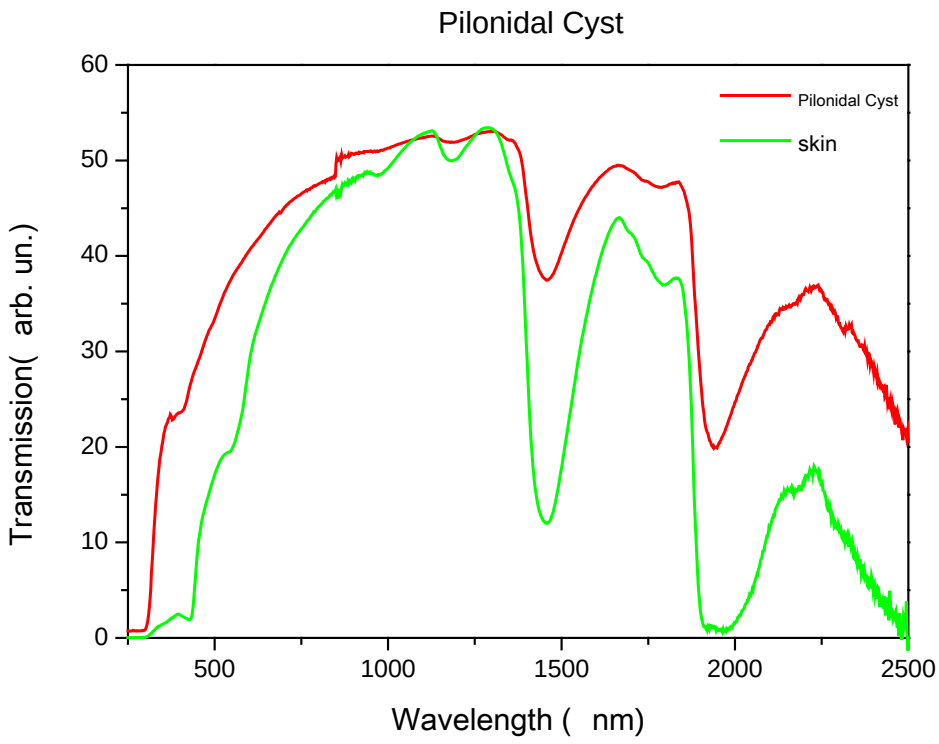

Figure 5.1. 5: Transmission of light as a function of wavelength obtained from pilonidal cyst

Our study has been continued by measuring and analyzing the transmission spectrum of pilonidal cyst that was surgically extracted from a twenty four year old man and underwent histological examination which reassured the clinical diagnosis. In addition to this, healthy skin from a nearby region has also been surgically extracted for comparison purposes, as always. The conclusions from Figure 5.1. 5 are that the differences between the two spectra are mainly located at the visible and

ultraviolet wavelength region. More specifically, from 200 nm to 450 nm healthy skin's spectrum is almost flat with the transmission close to zero and from 450 nm to 700 nm the transmission starts to increase. On the other hand, pilonidal cyst's graph exhibits a steep rise from 200 nm. The important finding is that in this case too detection of differences at the ultraviolet region apart from the visible and infrared regions can be detected for the transmission spectra between the two tissue cases. Furthermore, in this case where inflammatory skin (non cancerous cells) was the issue, the transmission spectrum exhibited a shape which differed from the healthy skin on one hand but also differed from the cancerous tissue cases. This constitutes the diagnostic method even more powerful as it proves to be able to diagnose and differentiate between various states of skin damage levels, i.e. fully healthy skin, skin with inflammation, and finally skin at a malignant state.

Nevus

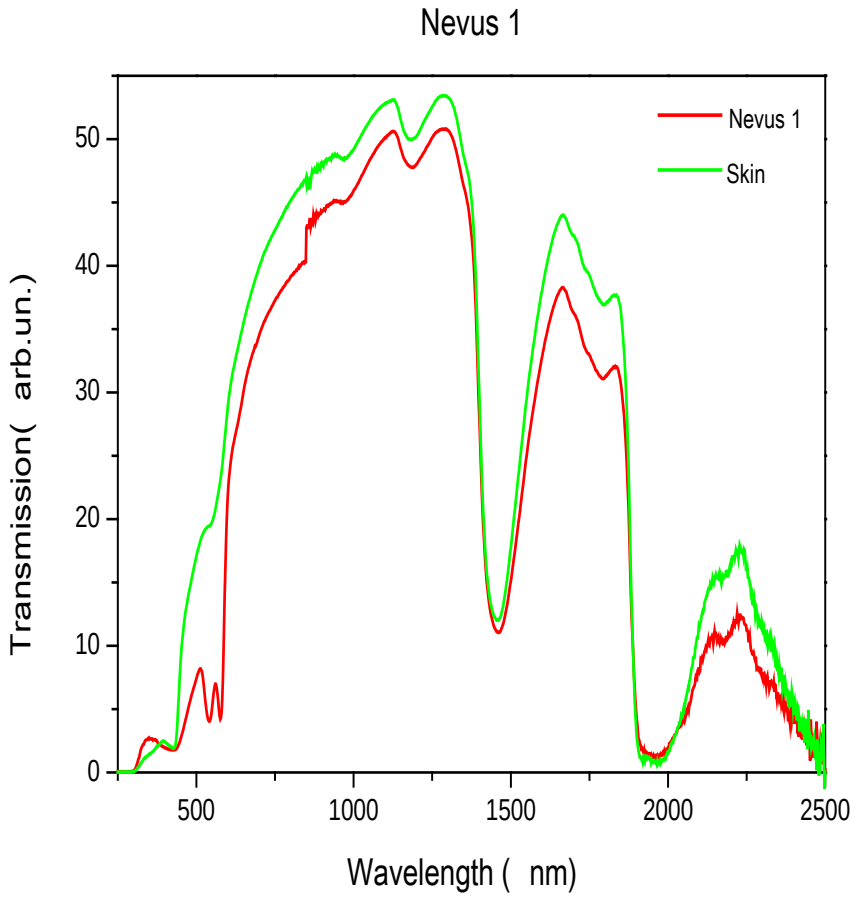

Figure 5.1. 6: Transmission of light as a function of wavelength obtained from nevus 1

The other kind of tissue that was examined in our experiments is nevus that was surgically extracted from a twenty one year old woman and was histologicaly examined. In addition to this, healthy skin from a nearby region has also been surgically extracted for comparison purposes. The main differences between the two spectra are detected in the visible light. More specifically, from 400 nm to 650 nm nevus' spectrum exhibits a fluctuating transmission with very low values. On the other hand, healthy skin's spectrum exhibits a monotonic rise as has also been observed at all previous transmission spectra. For the part of the spectrum with wavelengths larger than ~ 700 nm no considerable differences could be detected for the two spectra.

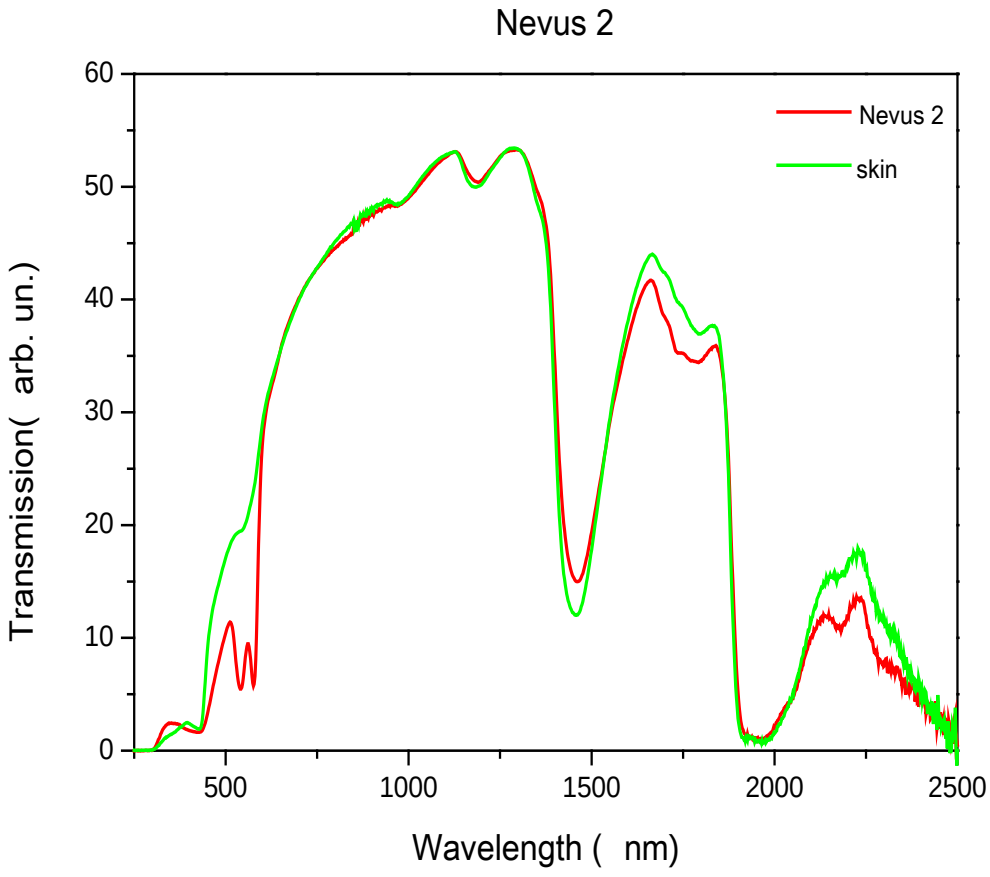

Figure 5.1. 7: Transmission of light as a function of wavelength obtained from nevus 2

A second nevus specimen was at our disposal that was surgically extracted from a forty three year old man and was histologicaly examined. In addition to this, healthy skin from a nearby region has also been surgically extracted for comparison purposes. The findings from this measurement resemble the ones we have from Figure 5.1. 6. More specifically, the main differences between the two spectra above are again located in the visible part of the spectrum. From 400 nm to 600 nm nevus' transmission spectrum exhibits fluctuations but on the other hand healthy skin's graph has a steady and monotonic rise.

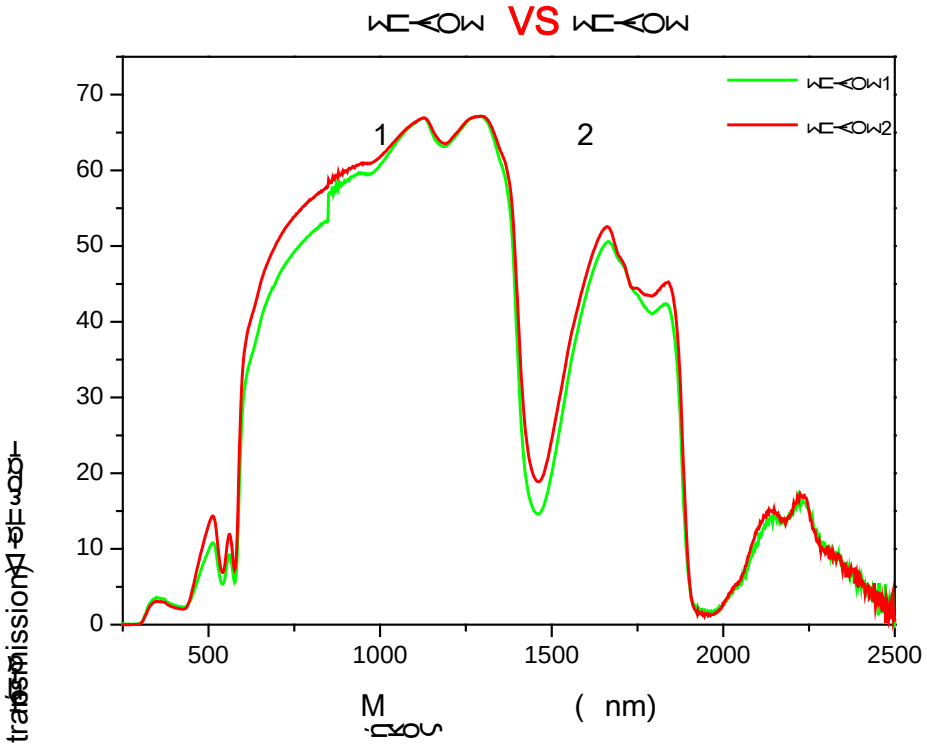

Figure 5.1. 8: Transmission of light as a function of wavelength of obtained from nevus 1 and 2

To sum up at Figure 5.1. 8 the spectrum of the two nevuses was examined. By comparing the two spectra it can be realized that these are almost the same as far as the form is concerned. Slight differences of the intensity of the transmission at some wavelengths are attributed to the different thickness of every tissue or generally variations in the morphological features and in the handling of the two samples. As a result, the fact that the method of transmission shown practically the same graph for

the same tissues proves the repeatability and reliability of the method. In addition to this, nevus constitutes a benign tumor and squamous cell carcinoma constitutes a malignant tumor. By comparing the absorption of nevus and squamous cell carcinoma it can be concluded that squamous cell carcinoma (cancer) exhibits specific transmission features at the visible and infrared part of the spectrum that no other non-cancerous tissues that have been examined possess.

Cornea/ Sclera

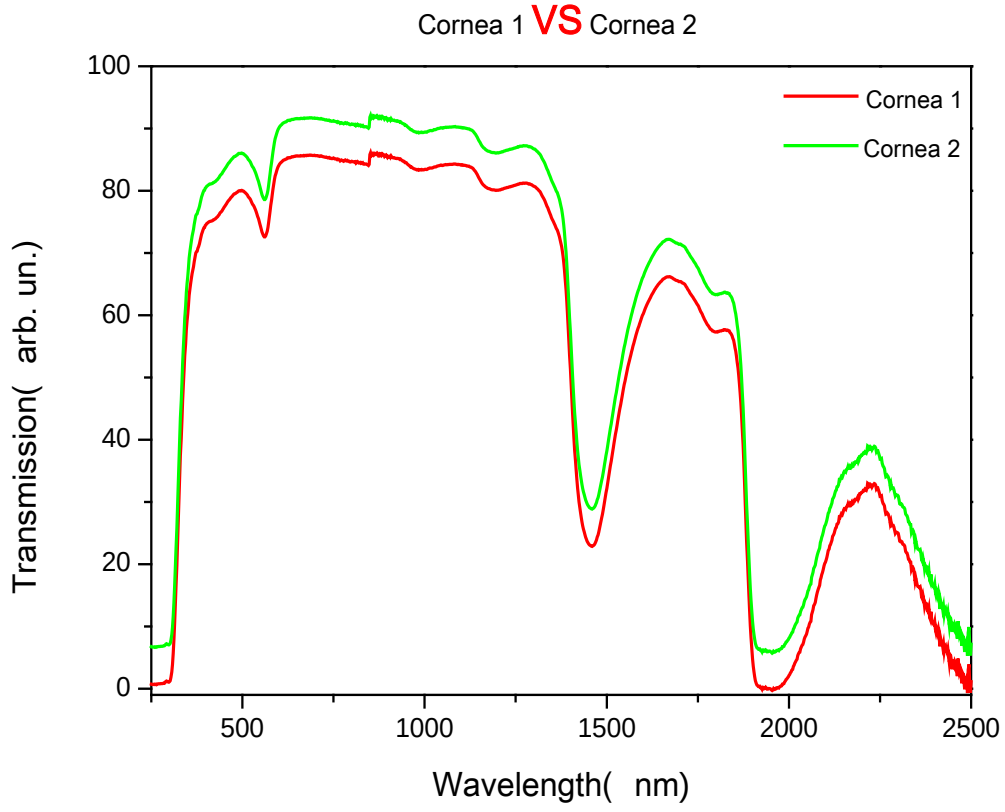

Figure 5.1. 9: Transmission of light as a function of wavelength of obtained from cornea 1 and 2

Figure 5.1. 9 shows and compares the transmission spectra from two healthy corneas from two different people that would be used for cornea transplant. By analysis of the two spectra no considerable differences are found. Slight intensity variations between the two spectra are attributed to differences in the thickness and other morphological differences that have been most probably introduced during surgical extraction due to imperfect cuts of the tissues and also due to possible differences in the handling of the two different samples during the spectral measurements. Consequently, this can be used as one more test case which further proves the repeatability and reliability of the transmission method in the diagnosis.

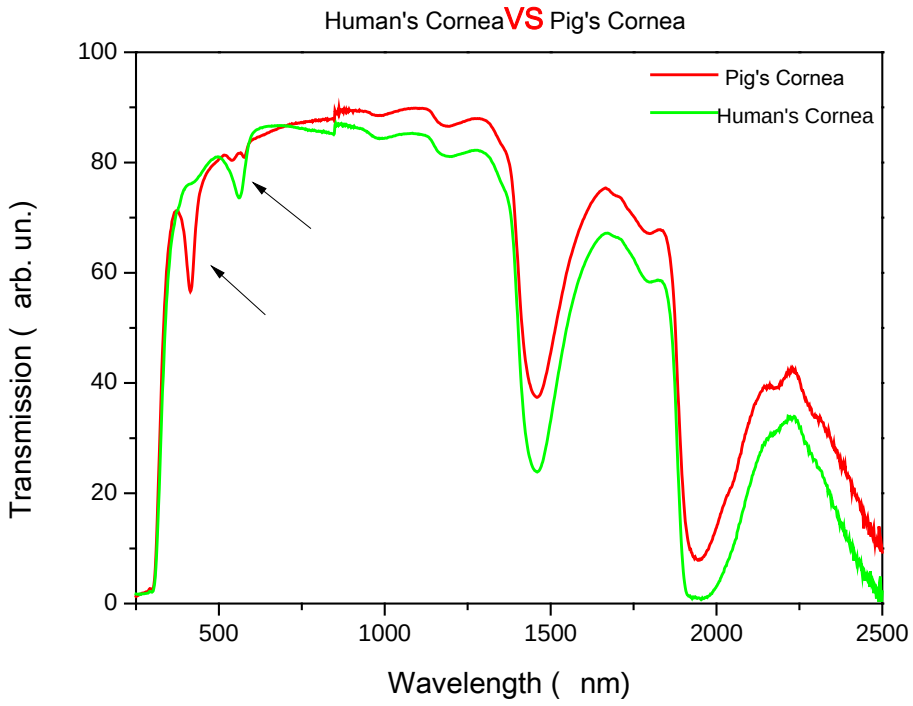

Figure 5.1. 10: Transmission of light as a function of wavelength obtained from human's and pig's cornea

At the next step of the study possible differences between human's and animal's tissues were investigated. More specifically, in Figure 5.1. 10 human's with pig's cornea have been compared. As the previous measurements, differences in the shapes of the transmission spectra is the point of interest. In this case obvious

differences can be seen in Figure 5.1. 10. Two sharp transmission dips can be observed at the wavelength of 478 nm and 611 nm for the case of pig's and human's cornea respectively. These two transmission dips are the major differentiation features which distinguish the transmission spectra between the pig's and the human corneas. The rest of the spectra present roughly the same shape for the two cases.

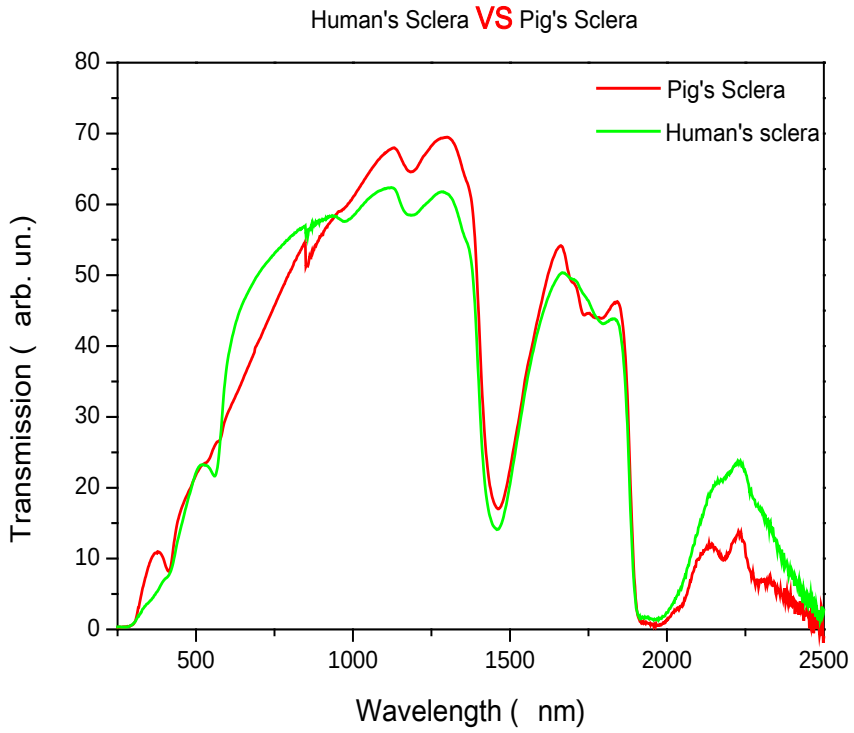

Figure 5.1. 11: Transmission of light as a function of wavelength obtained from human's and pig's sclera

Triggered by the cornea cases investigation was continued by cross examination of pig's vs. human scleras. This comparison is plotted in Figure 5.1. 11. As expected, the differences between the two graphs are found from 250 nm (ultraviolet) to 1100 nm (near infrared). It can be seen that the form of pig's sclera graph shows a steady ascent with two small descents until 1100 nm. On the other hand, the form of human's sclera graph has more steep changes.

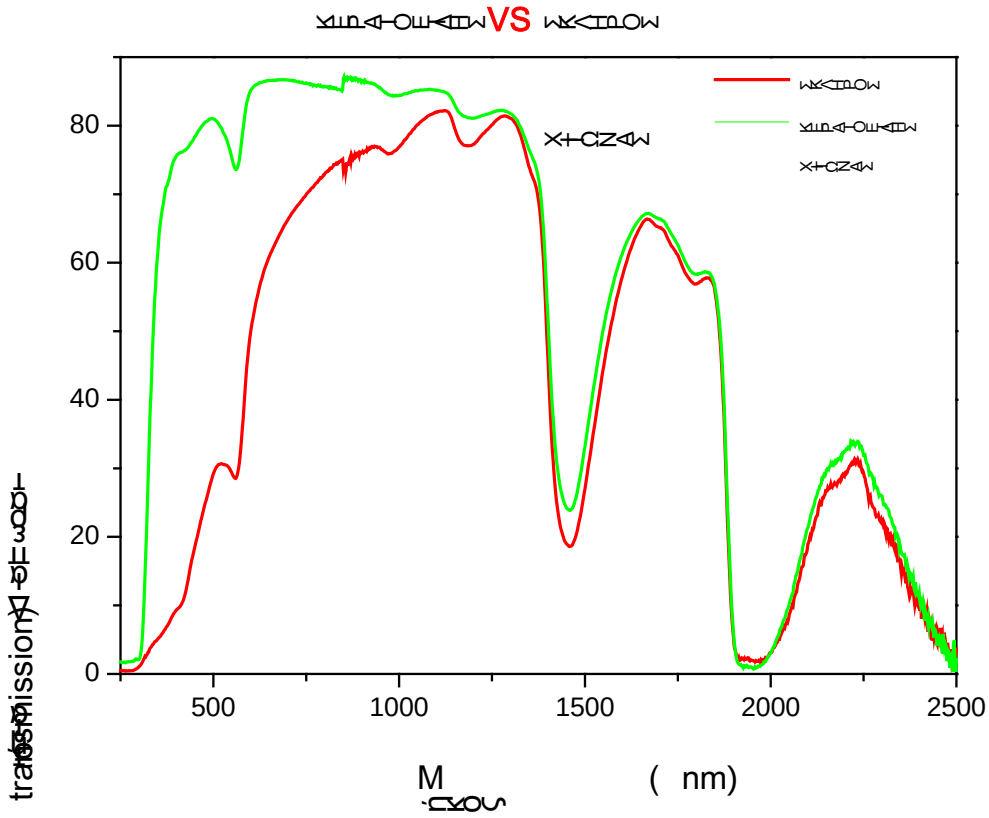

Figure 5.1. 12: Transmission of light as a function of wavelength obtained from human's cornea and sclera

At Figure 5.1. 12 two completely different kind of human eye tissues are compared. The first one is the cornea which allows light to pass through it and the second is the sclera which does not. The results of this comparison, shown in Figure 5.1. 12, is something that was anticipated. More specifically, the two spectra have a completely different form from 250 nm (ultraviolet) to 1100 nm (near infrared). In addition to this, as expected, the optically transparent eye tissue (cornea) shows consistently higher transmission values than the corresponding spectrum of sclera.

Pterygium

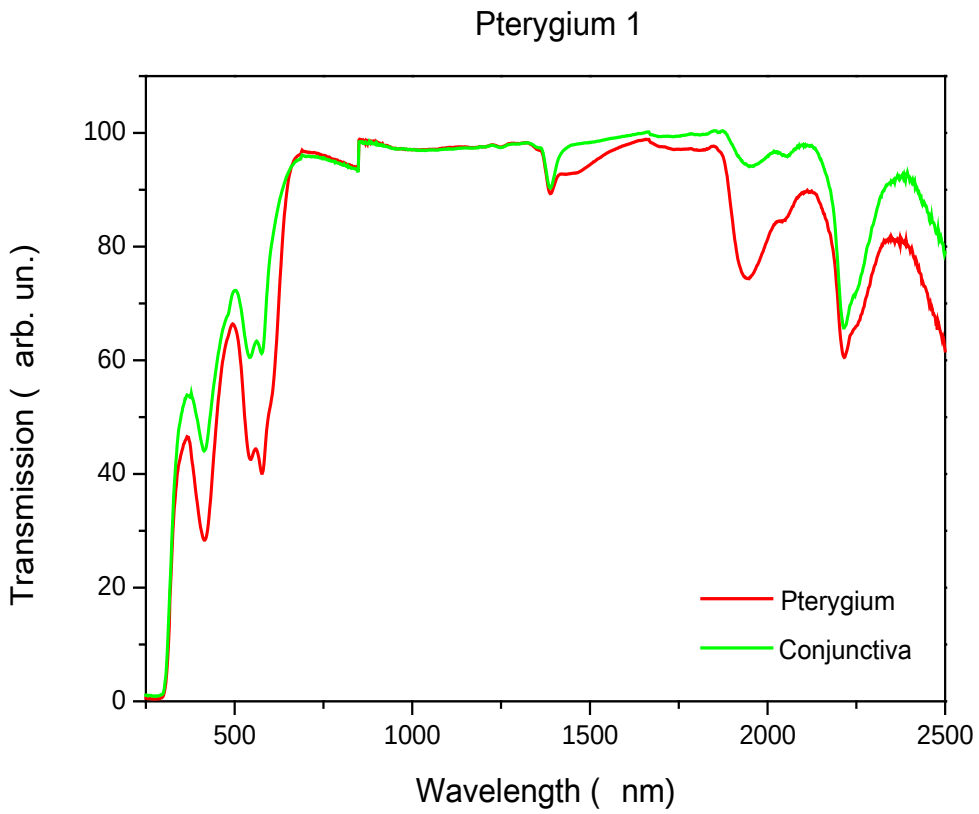

Figure 5.1. 13: Transmission of light as a function of wavelength obtained from pterygium 1

Lastly, comparisons of the conjunctiva (healthy tissue) of the eye with a series of pterygia (pathological tissue) have been examined with the transmission spectroscopy method. The first pterygium was surgically extracted by a sixty three year old man. By analyzing the two spectra shown in Figure 5.1. 13, no major differences were found in the region from 250 nm to 1000 nm. Nevertheless, the form of pterygium appears a decrease at 1350 nm to 1600 nm in contrast to conjunctiva.

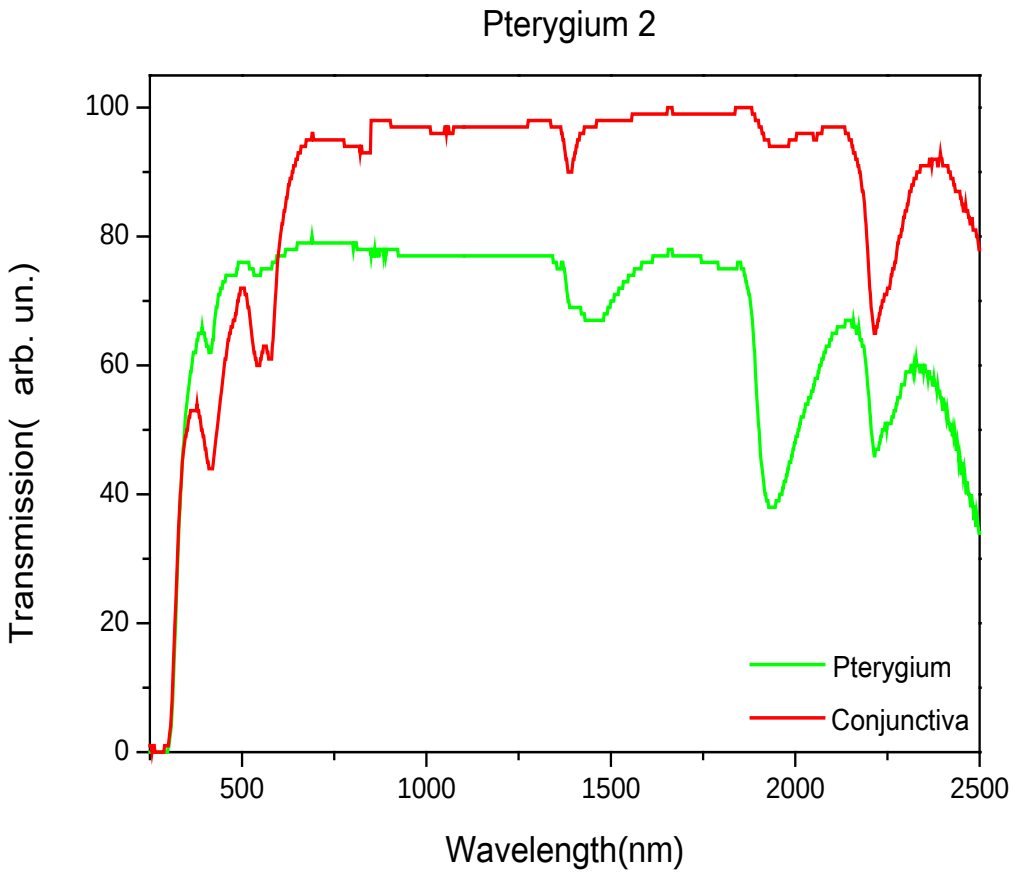

Figure 5.1. 14: Transmission of light as a function of wavelength ontained from pterygium 2

A second pterygium specimen was surgically extracted by a seventy one year old man. Unfortunately, as can seen in Figure 5.1. 14 the measurement exhibits significant noise from 600 nm to 2000 nm. Probably, this was caused because the samples were very small. Nevertheless, no important differences between the two spectra were detected.

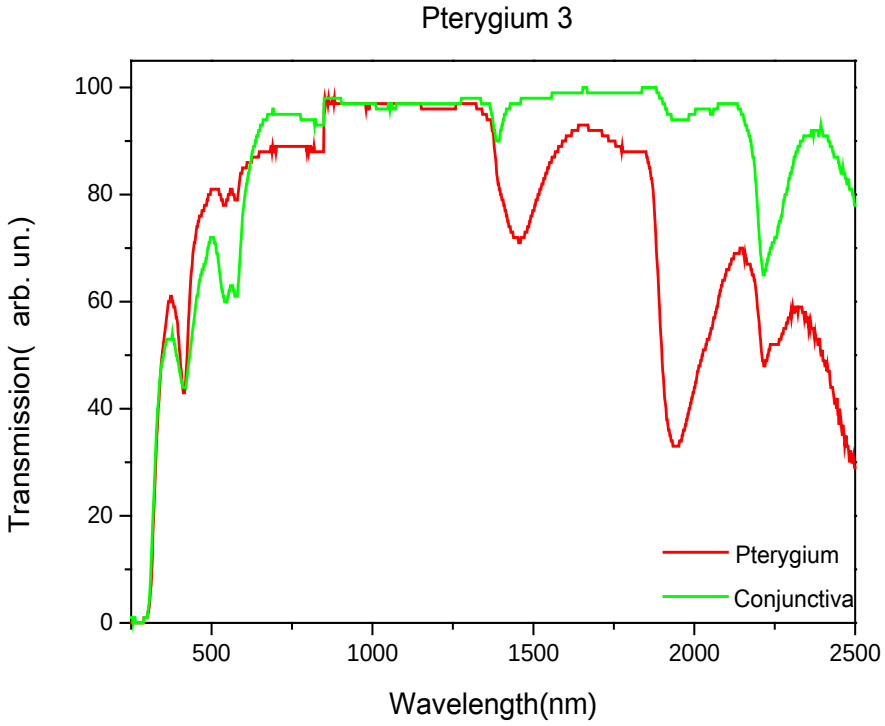

Figure 5.1. 15: Transmission of light as a function of wavelength obtained from pterygium 3

A third sample of pterygium was surgically extracted by a sixty seven year old woman. Unfortunately, as can be seen in Figure 5.1. 15 the measurement are again very noisy from 650 nm to 1800 nm. Probably, this was caused because the samples were very small and therefore difficult to handle and be placed properly inside the transmission spectroscopy apparatus. But as far as the small regions of wavelength where a good quality could be obtained no significant differences in the two spectra were detected.

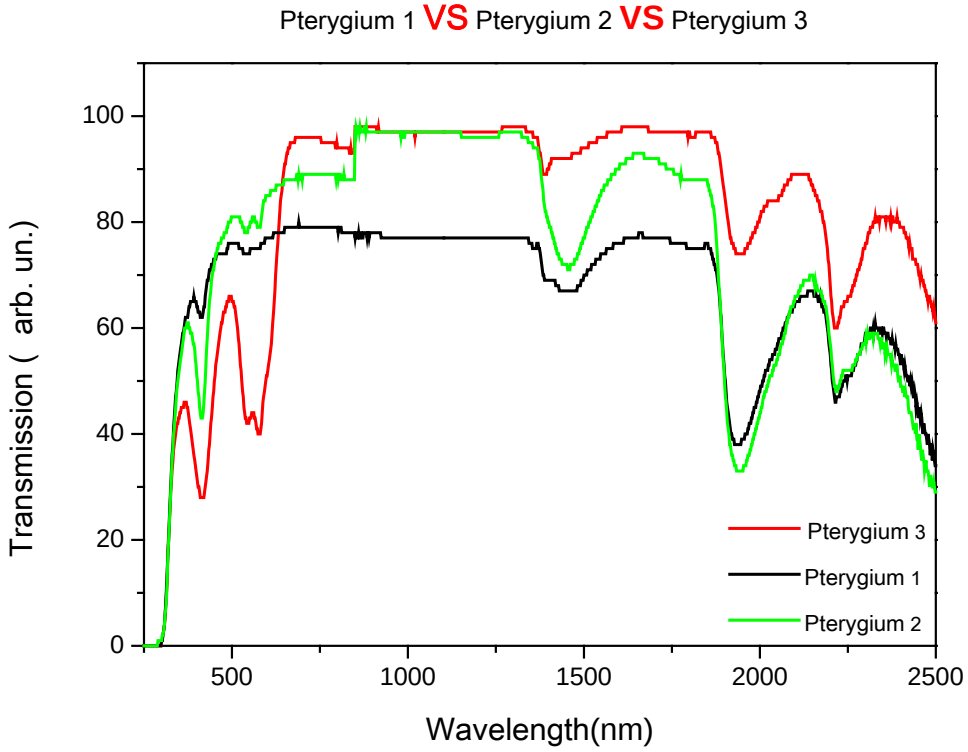

Figure 5.1. 16: Transmission of light as a function of wavelength obtained from pterygium 3

Eventually, comparison between all three pterygia is shown in Figure 5.1. 16. More specifically, from 200 nm to 600 nm and from 1600 nm to 2000 nm the three pterygiums have completely the same form of graphs. At the area of wavelength from 600 nm to 1600 nm reliable conclusions cannot be drawn because the quality of measurements is not good enough as has been stated above.

5.2.Fluorescence spectroscopy

Diagnostic techniques based on fluorescence spectroscopy have the potential to link the biochemical and morphologic properties of tissues to individual patient care. In particular, these techniques are fast, non-invasive and quantitative. Furthermore, they can be used to elucidate key tissue features, such as the cellular metabolic rate, vascular, intra-vascular oxygenation and alterations in tissue morphology. These tissue features can be interpreted to shed light on a variety of clinical problems, such as neoplasia. If applied successfully, fluorescence spectroscopy has the potential to represent an important step forward toward advances in diagnostic and therapeutic medical applications.

A typical fluorescence measurement of pilonidal cyst is shown in Figure 5.2. 1. In the y-axis the intensity of fluorescence is shown, while in the x-axis the wavelength is shown.

Pilonidal Cyst

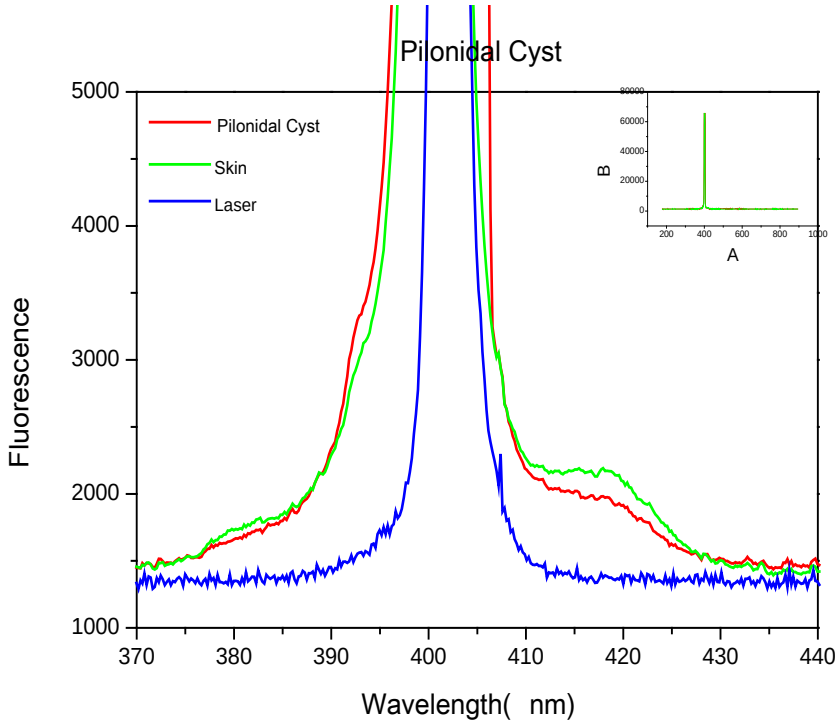

Figure 5.2. 1: Fluorescence of light as a function of wavelength obtained from pilonidal cyst

The pilonidal cyst that is demonstrated in Figure 5.2. 1 was surgically extracted from a twenty four year old man and was sent for histological examination which confirmed our clinical diagnosis. In addition to this, healthy skin which was near the pilonidal cyst was also surgically extracted. The pilonidal cyst used here for the fluorescence measurements is the same as the one used for the transmission measurements shown previously. In Figure 5.2. 1, the blue spectrum demonstrates the emission spectrum of the laser itself, the red one demonstrates the fluorescence spectrum obtained from the pilonidal cyst and the green one demonstrates the fluorescence spectrum obtained from the healthy skin. The fluorescence spectra for both the pilonidal cyst and the healthy tissue exhibit increased intensity than the laser spectrum at regions outside the emission spectrum of the laser itself, i.e. at the regions 375-390 nm and 410-430 nm. This increased emission shows the contribution of tissue, either healthy or inflammatory. However the differences in the fluorescence

spectra between the healthy skin and the pinodal cyst are minimal and at the limits of the accuracy of the measurements. Therefore, no conclusion can be drawn on the capability of this technique to distinguish the healthy tissue form the inflammatory one.

Nevus

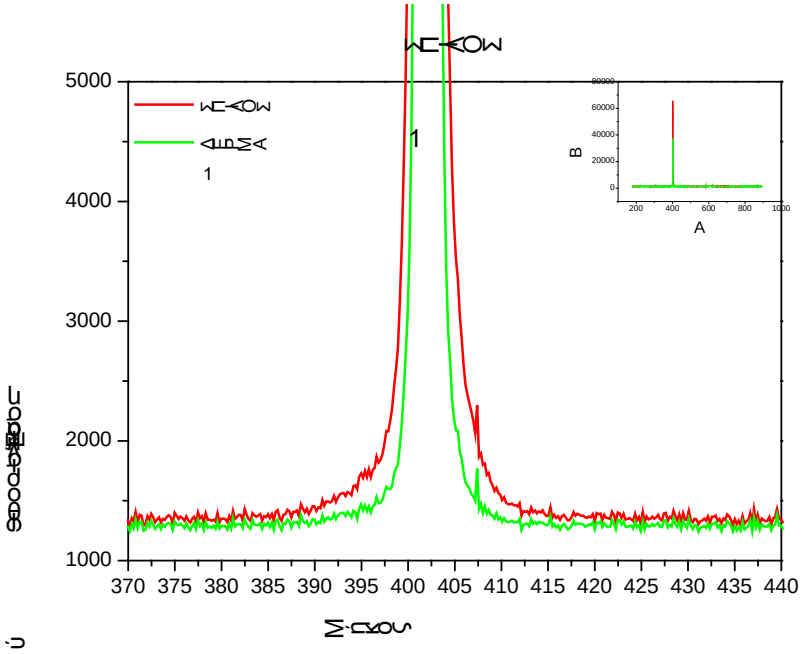

Figure 5.2. 2: Fluorescence of light as a function of wavelength obtained from nevus 1

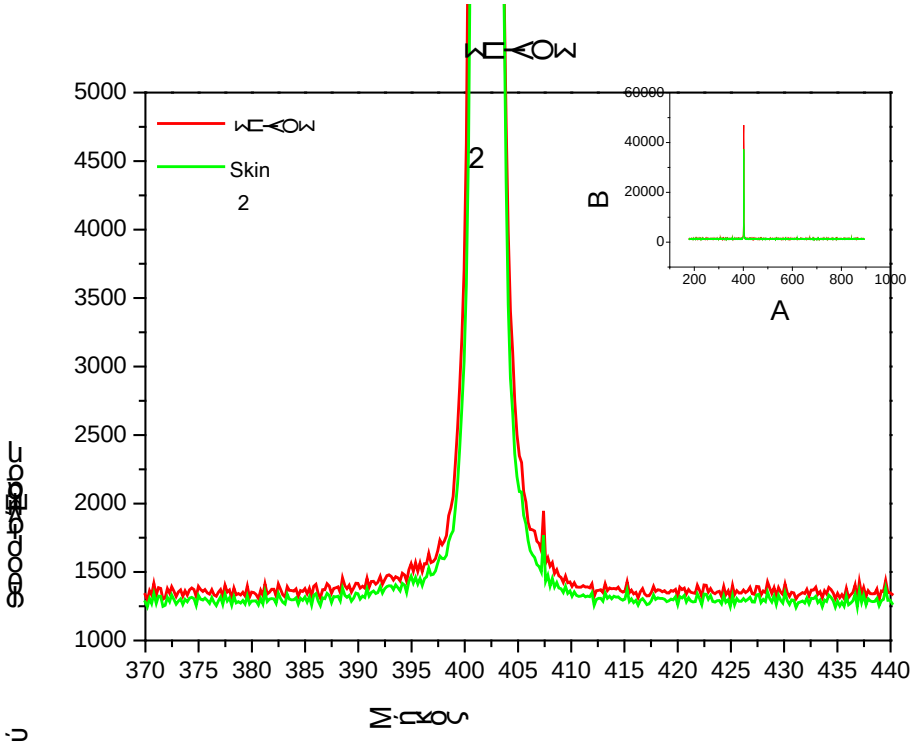

Figure 5.2. 3: Fluorescence of light as a function of wavelength obtained from nevus 2

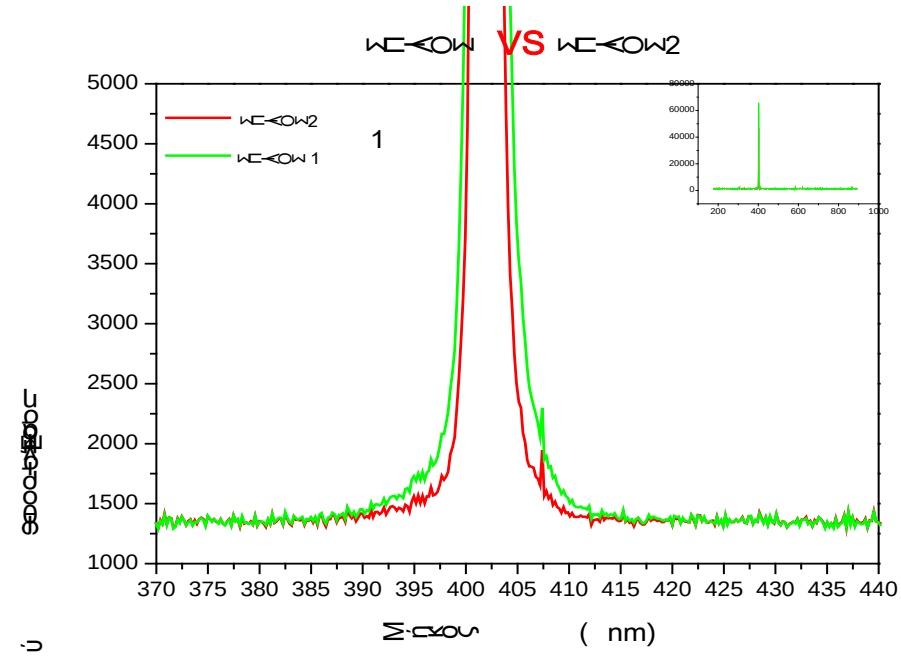

Figure 5.2. 4: Fluorescence of light as a function of wavelength obtained from nevus 1 and 2

Afterwards a measurement of the fluorescence of the two nevuses followed. The same nevuses were also examined at transmission mode. As can be seen in Figure 5.2. 2, Figure 5.2. 3 and Figure 5.2. 4 the form of the spectra are almost the same and they only have minor differences (the form of nevus has a slightly higher fluorescence intensity in contrast to skin). Eventually, from the comparison of these three graphs there are no significant differences as far as the form of the spectra are concerned. As a result, from these measurements it is not feasible to draw reliable conclusions.

Eye Tissues

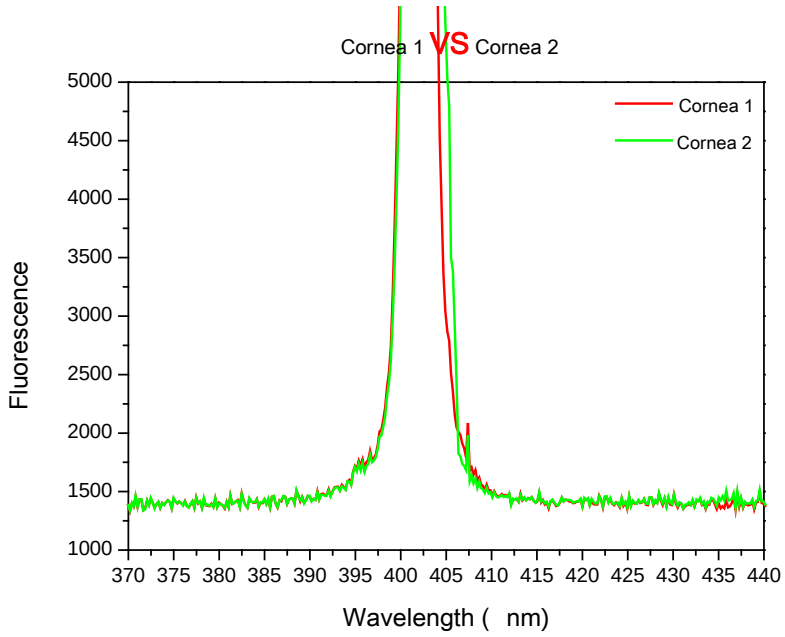

Figure 5.2. 5: Fluorescence of light as a function of wavelength obtained from cornea 1 and 2

At the next step of the experiment the rest of the eye tissues were examined. At the beginning two different healthy corneas were compared. The same corneas were referred above at the measurements of absorption. At this measurement, the two graphs have a common point where they meet at 406 nm. As far as the rest form of the two spectra is concerned they look alike. That was something that was anticipated because two different tissues that have the same structure were compared.

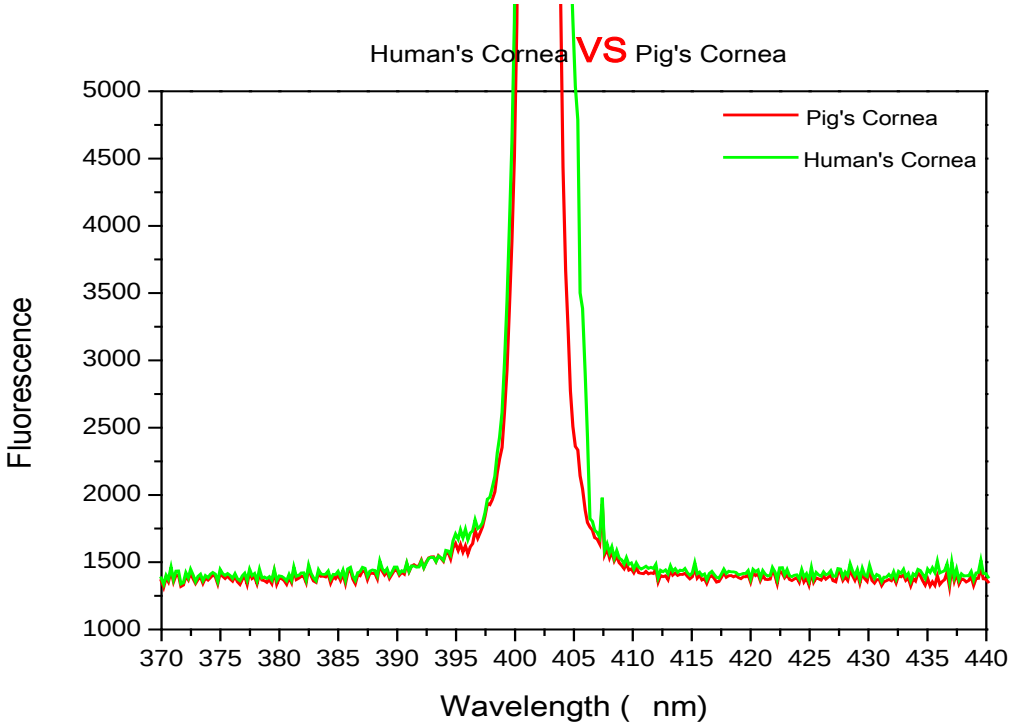

Figure 5.2. 6: Fluorescence of light as a function of wavelength obtained from human's and pig's cornea

Then tissues and especially corneas from different species were compared, one from human and one from pig. The same tissues were referred above at the measurements of absorption. In this measurement, the green spectrum demonstrates human's cornea and the red one demonstrates pig's cornea. By analysis of the two spectra of Figure 5.2. 6 the conclusion is that the form of pig's cornea spectrum has a more steep descent from 404 nm to 407 nm but not any outstanding difference.

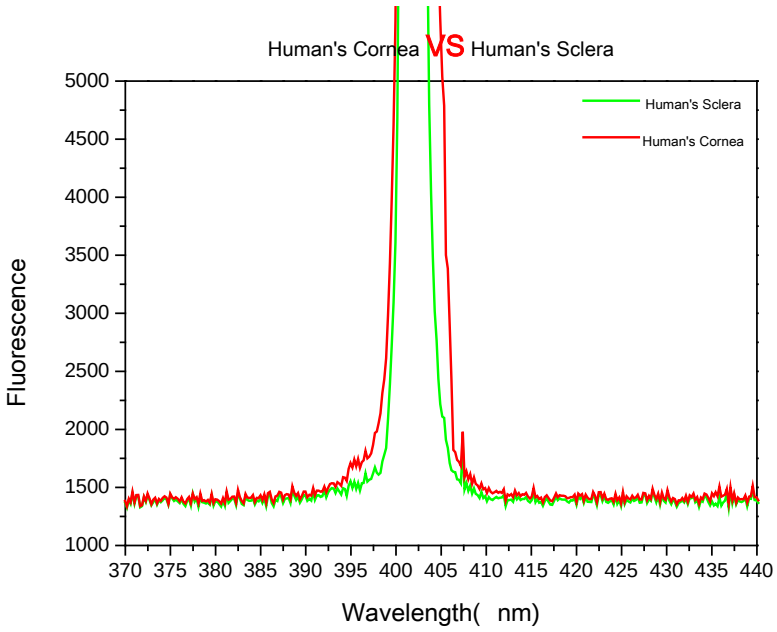

Figure 5.2. 8: Fluorescence of light as a function of wavelength obtained from cornea and sclera

At Figure 5.2.8 the fluorescence of two different kind of tissues of the eye, and especially human's cornea with human's sclera were compared. The same tissues were referred above at the measurements of absorption. In this measurement, the green line shows the fluorescence spectrum of human's sclera and the red line shows human's cornea respectively. By checking the two spectra it is noticeable that the form of human's sclera graph has a more steep decrease from 404 nm to 407 nm.

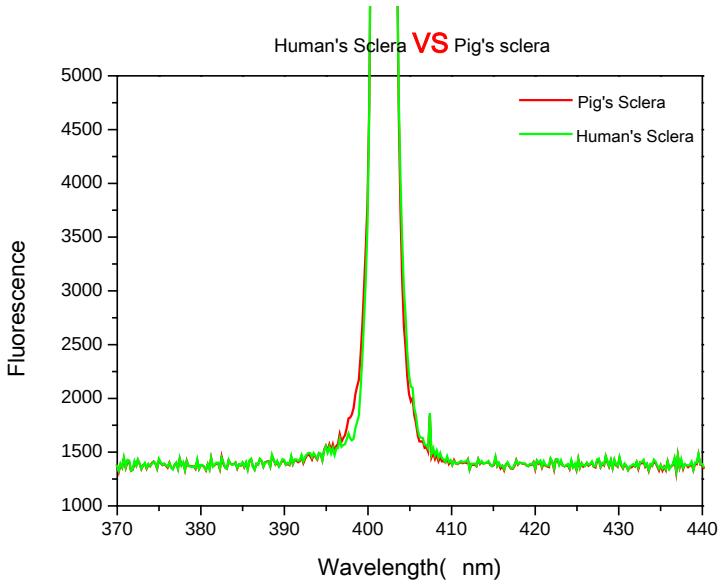

Figure 5.2. 9: Fluorescence of light as a function of wavelength obtained from human's and pig's sclera

Finally tissues, and especially sclera, from different species were compared; one from human and one from pig. These tissues were used above at the measurements of transmission. In this measurement, the green line demonstrates the spectrum for human's sclera and the red line demonstrates the spectrum for pig's cornea. At this case, it is obvious that the two spectra are similar and in large spectral regions the two graphs overlap with each other.

6.Conclusions And Perspectives

In summary, the presented experiments show that transmission and fluorescence spectroscopy can be a powerful diagnostic technique for the detection of pathology/neoplastic growth in a variety of epithelial tissues. The use of absorption and particularly fluorescence spectroscopy for the characterization of pathology/neoplastic and non-neoplastic tissues, *in vivo* has only recently began to evolve. To improve the role of these techniques in clinical applications, several issues have yet to be addressed fully. Evaluation of the clinical investigations performed within and between different tissue sites indicates that there is a considerable variability in the implementation of this technology. In particular for fluorescence spectroscopy, the variability arises from the selection of excitation and emission wavelengths, probe geometry and the method of analysis of the spectral information. To select the optimal excitation and emission wavelengths, it is necessary to be able to measure the fluorescence of tissues, at multiple excitation and emission wavelengths in the ultraviolet and visible spectral regions.

The optimization of the probe geometry and the method of analysis has been somewhat limited by the fact that the underlying biochemical and morphologic features that give rise to differences in the transmission and fluorescence spectra measured from pathological/neoplastic and healthy/non-neoplastic tissues has not been rigorously quantified for all tissue types. In order to overcome this obstacle further investigations should be carried out in order to identify the diagnostically fluorescent micro-structures that contribute to the tissue fluorescence emission spectra and the optimal probe geometry that can maximally exploit these features. Animal models are useful with regard to developing methodologies that can be used to elucidate the biochemical and morphologic properties of tissue and optimizing the instruments to exploit these features. The advantages they offer are:

1) They are well-established,

2) Spectral measurements can be made per tissue site for a variety of experimental and biologic conditions and

3) Data can be obtained from a statistically significant number of animals for the purpose of validation, without the need for expensive clinical trials.

To sum up:

1. Absorption spectroscopy in transmission mode is a powerful diagnostic method which can detect pathological differences in a wide optical spectrum extending from the near UV to the Visible and the near infrared.
2. Absorption spectroscopy has higher sensitivity and specificity in comparison with fluorescence spectroscopy. The later needs further improvements in order to provide unambiguous feedback for the pathological status of tissues.
3. The presented methods can be possibly further upgraded and tuned in order to develop noninvasive diagnostic tools by performing the diagnosis in vivo.

References

1) Jan Kazimierz Danysz, Le Radium 9, 1 (1912); 10, 4 (1913)

2) *"mass spectrometer" (PDF). 2009. doi:10.1351/goldbook.M03732.*

3) *Cassin, B.; Solomon, S. (1990). Dictionary of Eye Terminology. Gainesville, Florida: Triad Publishing Company.*

4) *Goldstein, E. Bruce (2007). Sensation & Perception (7th ed.). Canada: Thompson Wadsworth.*

5) *Najjar, Dany. "Clinical optics and refraction".*

6) *"Why does the cornea need oxygen?". The Association of Contact Lens Manufacturers.*

7) *Nees, David W.; Fariss, Robert N.; Piatigorsky, Joram (2003). "Serum Albumin in Mammalian Cornea: Implications for Clinical Application". Investigative Ophthalmology & Visual Science.* ***44*** *(8): 3339–45. doi:10.1167/iovs.02-1161. PMID 12882779*

8) *Romer, Alfred Sherwood; Parsons, Thomas S. (1977). The Vertebrate Body. Philadelphia: Holt-Saunders International. pp. 461–2. ISBN 0-03-910284-X.*

9) Mosby's Medical, Nursing & Allied Health Dictionary, Fourth Edition, Mosby-Year Book Inc., 1994, p. 1402

10) Cassin, B. and Solomon, S. *Dictionary of Eye Terminology*. Gainesville, Florida: Triad Publishing Company, 1990.

11) Hermann D. Schubert. *Anatomy of the Orbit*
http://www.nyee.edu/pdf/schubert.pdf

12) eye, human."Encyclopædia Britannica from Encyclopædia Britannica 2006 Ultimate Reference Suite DVD 2009

13) *Romer, Alfred Sherwood; Parsons, Thomas S. (1977). The Vertebrate Body. Philadelphia, PA: Holt-Saunders International. p. 461.* ISBN 0-03-910284-X.

14) *Coroneo, MT (November 1993). "Pterygium as an early indicator of ultraviolet insolation: a hypothesis". Br J Ophthalmol. **77** (11): 734–9.*

15) *Kunimoto, Derek; Kunal Kanitkar; Mary Makar (2004). The Wills eye manual: office and emergency room diagnosis and treatment of eye disease. (4th ed.). Philadelphia, PA: Lippincott Williams & Wilkins. pp. 50–51. ISBN 978-0781742078.*

16) *Gulani, A.C. (24 March 2005). "Extended Sun Exposure Increases Risk of Eye Pterygium".*

17) *Fisher, J.P.; Trattler, W.B. (12 January 2009). "Pterygium".*

18) *Klintworth, G; Cummings, T. "24; The eye and ocular adnexa". In Stacey, Mills. Sternberg's Diagnostic Surgical Pathology (5th ed.). ISBN 978-0-7817-7942-5.*

19) http://www.paramountbooks.com.pk/LoginIndex.asp?title=Concise-Ophthalmology-(pb)-2014&Isbn=9789696370017&opt=3&sUBcAT=06

20) *Gulani, A; Dastur, YK (Jan–Mar 1995). "Simultaneous pterygium and cataract surgery.". Journal of postgraduate medicine. **41** (1): 8–11. PMID 10740692. Retrieved 30 November 2012.*

21) *GBD 2013 Mortality and Causes of Death, Collaborators (17 December 2014). "Global, regional, and national age-sex specific all-cause and cause-specific mortality for 240 causes of death, 1990-2013: a systematic analysis for the Global Burden of Disease Study 2013.". Lancet. **385**: 117–71. doi:10.1016/S0140-6736(14)61682-2. PMC 4340604. PMID 25530442.*